Quantum transport through mesoscopic disordered interfaces, junctions, and multilayers

2002 J. Phys.: Condens. Matter 14 7871

(http://iopscience.iop.org/0953-8984/14/34/307)

INSTITUTE OF PHYSICS PUBLISHING JOURNAL OF PHYSICS: CONDENSED MATTER

J. Phys.: Condens. Matter **14** (2002) 7871–7899 PII: S0953-8984(02)36538-X

Quantum transport through mesoscopic disordered interfaces, junctions, and multilayers

Branislav K Nikolić[1]

Department of Physics and Astronomy, SUNY at Stony Brook, Stony Brook, NY 11794-3800, USA

Received 2 May 2002
Published 15 August 2002
Online at stacks.iop.org/JPhysCM/14/7871

Abstract

This study explores perpendicular transport through macroscopically inhomogeneous three-dimensional disordered conductors using mesoscopic methods (the real-space Green function technique in a two-probe measuring geometry). The nanoscale samples (containing ∼1000 atoms) are modelled by a tight-binding Hamiltonian on a simple cubic lattice where disorder is introduced in the on-site potential energy. I compute the transport properties of: disordered metallic junctions formed by concatenating two homogeneous samples with different kinds of microscopic disorder, a single strongly disordered interface, and multilayers composed of such interfaces and homogeneous layers characterized by different strengths of the same type of microscopic disorder. This allows us to: contrast the resistor model (semiclassical) approach with a fully quantum description of dirty mesoscopic multilayers; study the transmission properties of dirty interfaces (where the Schep–Bauer distribution of transmission eigenvalues is confirmed for a single interface, as well as for a stack of such interfaces that is thinner than the localization length); and elucidate the effect of coupling to ideal leads ('measuring apparatus') on the conductance of both bulk conductors and dirty interfaces. When a multilayer contains a ballistic layer in between two interfaces, its disorder-averaged conductance oscillates as a function of the Fermi energy. I also address some fundamental issues in quantum transport theory—the relationship between the Kubo formula in the exact state representation and the 'mesoscopic Kubo formula' (which gives the exact zero-temperature conductance of a finite-size sample attached to two semi-infinite ideal leads) is thoroughly re-examined by comparing their outcomes for both the junctions and homogeneous samples.

[1] Present address: Department of Physics, Georgetown University, Washington, DC 20057-0995, USA.

0953-8984/02/347871+29$30.00

1. Introduction

The experimental discovery [1, 2] of a giant-magnetoresistance (GMR) phenomenon has revived interest in the transport properties of macroscopically inhomogeneous conductors, such as metallic junctions [3] and multilayers [4]. Furthermore, unusual systems for traditional transport theory, like single dirty interfaces [5] which are ubiquitous elements in such circuits, have entailed the introduction of new concepts to replace usual quantities (e.g., mean free path ℓ) used to describe transport in bulk samples. Although some of these problems were formulated long ago within the (semiclassical) transport theory [6–8], new attacks have employed all (quantum and semiclassical) transport formalisms developed thus far, revealing that such problems are by no means resolved [4, 9]. In particular, the re-examination of various fundamental issues in transport theory has been brought about by the experimental and theoretical advances in mesoscopic physics [10]. Thus, the Landauer–Büttiker scattering formalism [11] has been frequently invoked to study transport in both non-magnetic [12] and magnetic multilayered conductors [13, 14]. Obviously, the thorough understanding of transport properties due to purely *multilayer + disorder* effects is a prerequisite for the analysis of more complicated phenomena in inhomogeneous structures.

Besides providing the means to compute the (quantum) conductance of finite-size samples, mesoscopic methods give additional physical insight by delineating transmission properties of the sample. The finite size of mesoscopic systems plays an important role in determining the conductance through the scattering approach, but no further limitations exist—the exactness of results obtained in this manner is heavily exploited throughout the paper. Practical realization of this programme appears in different incarnations, i.e., different Landauer-type [15] or Kubo [16] formulae for a finite-size phase-coherent sample attached to semi-infinite ideal (disorder-free) leads. These prescriptions are usually made computationally efficient by combining them with some Green function technique [17, 18].

Here I employ mesoscopic quantum transport methods to calculate the conductance of disordered samples which are macroscopically inhomogeneous, i.e., composed of different homogeneous conductors ('layers') joined through some interfaces ('monatomic layers'). In homogeneous conductors, whose properties have been well studied throughout the history of localization theory [19], impurities generate only microscopic inhomogeneity on the scale $\sim\lambda_F$ (Fermi wavelength). Our goal is twofold:

(1) Most mesoscopic studies have been focused on the bulk homogeneous conductors [18] in the weak scattering transport regime. Only recently have systems such as metallic multilayers [12] or single dirty interfaces [5, 20] been tackled in this manner. By employing non-perturbative numerical methods we can access strongly disordered junctions, single strongly disordered interfaces (when stacked together to form a bulk conductor, our interfaces would form an Anderson insulator), and multilayers composed of such interfaces and bulk diffusive or ballistic mesoscopic conductors. A system is called mesoscopic if its size L is smaller than the dephasing length L_ϕ, which is a typical distance for an electron to travel without losing its phase coherence ($L_\phi \lesssim 1$ μm in current low-temperature experiments), and is therefore determined by decoherence processes caused by the coupling to the environment either through inelastic scattering (electron–electron and electron–phonon) or just by the change of the environment quantum state (e.g., spin-flip scattering from a magnetic impurity). The term metallic implies that the conductance G of a bulk homogeneous sample is much larger than the conductance quantum $G_Q = 2e^2/h$. For interfaces one needs a different nomenclature: they are termed 'dirty' [5] if their conductance G/G_Q is much smaller than the number of conducting channels $N_{\rm ch}$ ($N_{\rm ch} \sim k_F^2 S$ in three dimensions, with $k_F = 2\pi/\lambda_F$, and S is the cross-

section of a sample). Lacking a better language, I denote the multilayers studied here as 'dirty metallic', meaning that scattering is due to a random potential and their conductance is $G_M \ll G_Q N_{\rm ch}$. Nevertheless, layer components are chosen to be metallic $G \gg G_Q$, and are well described, in the diffusive limit $L \gg \ell$, by semiclassical transport theory [21]. In terms of material parameters, the resistivity of a bulk homogeneous material, from which nanoscopic layers are cut out, is few 100 $\mu\Omega$ cm, which is typical of dirty transition metal alloys. Thus, the possible small conductance of layers is not necessarily caused by approaching the localization–delocalization transition [22] upon increasing disorder, as is usual in homogeneous bulk samples. The conductors are modelled by a tight-binding Hamiltonian (TBH) with on-site potential disorder. This corresponds to a model of free electrons (understood here as Landau quasiparticles with parameters renormalized by both band structure effects and Fermi liquid interaction) with random point scatterers [9], which is used frequently in studies of similar systems. While isotropic scattering sets semiclassical vertex corrections to zero (which are determined by ladder diagrams [23] generating the difference between momentum relaxation time and elastic mean free time, or the scattering-in term in the Boltzmann theory), it does not eliminate the higher-order quantum interference vertex corrections. These terms are non-local on the mesoscopic length scale L_ϕ, and therefore invalidate [4] the concept of local position-dependent conductivity $\sigma(x)$ as the usual way of describing the multilayered structures (in semiclassical approximation) [9]. Since I exploit here exact techniques, all quantum localization effects which are not necessarily small in dirty systems [9, 21] are included from the outset. All three types of sample are studied for electron transport perpendicular to the layers (or interfaces), which is the so-called current-perpendicular-to-plane (CPP) geometry [4]. Once the disorder-averaged resistance of the multilayer is computed, we can compare it to the resistance given by the resistor model [24], (i.e., a sum of the bulk layers and interface resistances connected like classical ohmic resistors in a series).

(2) I investigate some fundamental issues in the quantum transport theory using dirty metallic junctions as described above as a testing ground, as well as homogeneous disordered samples as a reference. That is, I compare the transport properties computed from the Kubo formula in the exact single-particle state representation (which was widely used [25] in the 'premesoscopic' era [26] of the Anderson localization theory) and the 'mesoscopic Kubo formula' for the open finite-size system attached to two ideal leads [16]. In the former case the system is closed and the eigenproblem of the Hamiltonian is solved exactly by numerical diagonalization, while in the latter case energy levels of a sample are broadened by the coupling to the leads, and I use real-space Green functions for such an open sample plugged into the Kubo formula [16] (which is then equivalent to the Landauer two-probe formula [27]) to get its conductance. Also, the influence of the leads ('measuring apparatus') and the lead–sample coupling on the conductance (which is akin to the problems encountered in quantum measurement theory [28]) is explicitly quantified.

The paper is organized as follows. Section 2 deals with some general remarks on the Kubo linear response formalism and current conservation. This should serve as a guide for proper application of Kubo formulae on the finite-size systems. In section 3, the Kubo formula in exact state representation is compared to the Kubo formula for the finite-size sample by evaluating them for dirty metallic junctions, as well as for homogeneous samples. Section 4 presents the results on the transmission properties, and conductance derived from them, of a single dirty interface as well as thin layers composed of few such interfaces. The calculations are completed in section 5 by examining different types of multilayer, containing disordered and/or ballistic layers concatenated through the interfaces described in section 4. Section 6

provides a summary of the technical results, emphasizing physical insights gained from them.

2. Kubo formulae and current conservation

The basic global transport property, for small applied voltage, is linear conductance (or equivalent resistance $R = 1/G$). The conductance G is defined by the Ohm's law:

$$I = GV, \tag{1}$$

relating the current I to the voltage drop V. Since this is a plausible relation for a linear transport regime, more information is contained in the local form of the Ohm's law:

$$\boldsymbol{j}(\boldsymbol{r}, \omega) = \int \mathrm{d}\boldsymbol{r}'\, \underline{\sigma}(\boldsymbol{r}, \boldsymbol{r}'; \omega) \cdot \boldsymbol{E}(\boldsymbol{r}', \omega). \tag{2}$$

In what follows, the focus will be on the DC transport $\omega \to 0$. Although it is possible to treat $\boldsymbol{E}(\boldsymbol{r})$ as an externally applied electric field and then include the effects of Coulomb interaction between electrons as a contribution to the vertex correction [4], the usual approach is to use the total (local and inhomogeneous) electric field $\boldsymbol{E}(\boldsymbol{r}) \equiv \boldsymbol{E}_{\mathrm{loc}}(\boldsymbol{r}) = -\boldsymbol{\nabla}\mu(\boldsymbol{r})/e$, which is the sum of external field plus the field due to the charge redistribution from the system response [45]. The electrons are then treated as independent quasiparticles. The electrochemical potential μ in non-equilibrium situations (like transport) is not a well-defined quantity, and can serve only, e.g., to parametrize the carrier population [29]. The relation (2) defines the meaning of the non-local conductivity tensor (NLCT) $\underline{\sigma}(\boldsymbol{r}, \boldsymbol{r}')$ as the fundamental microscopic quantity in the linear response theory. This quantity gives the current response at $\boldsymbol{r}$ due to an electric field at $\boldsymbol{r}'$. The requirement of current conservation in the DC transport

$$\boldsymbol{\nabla} \cdot \boldsymbol{j}(\boldsymbol{r}) = 0, \tag{3}$$

coupled to equation (2) and together with appropriate boundary conditions at infinity or possible interfaces [30], makes it possible to find $\boldsymbol{E}(\boldsymbol{r})$. The conductance (power dissipated by the voltage V squared) is then given by

$$G = \frac{1}{V^2}\int_\Omega \mathrm{d}\boldsymbol{r}\, \boldsymbol{E}(\boldsymbol{r}) \cdot \boldsymbol{j}(\boldsymbol{r}) = \frac{1}{V^2}\int_\Omega \mathrm{d}\boldsymbol{r}\, \mathrm{d}\boldsymbol{r}'\, \boldsymbol{E}(\boldsymbol{r}) \cdot \underline{\sigma}(\boldsymbol{r}, \boldsymbol{r}') \cdot \boldsymbol{E}(\boldsymbol{r}'), \tag{4}$$

where Ω is the sample volume, and at first sight appears to require knowledge of local electric fields within the sample. However, it was shown in the course of recent re-examination of transport theory [31], driven by the problems of mesoscopics, that current conservation imposes stringent requirements on the form of the NLCT:

$$\boldsymbol{\nabla} \cdot \underline{\sigma}(\boldsymbol{r}, \boldsymbol{r}') = \underline{\sigma}(\boldsymbol{r}, \boldsymbol{r}') \cdot \boldsymbol{\nabla}' = 0, \tag{5}$$

where absence of magnetic field is assumed to get this special case of a more general theorem [27]. This allows us to use arbitrary electric field factors in equation (4), including $\boldsymbol{E}(\boldsymbol{r}) \neq \boldsymbol{E}(\boldsymbol{r}')$ (a homogeneous field $E = V/L$ across a sample of length L is usually assumed in the textbook literature [23]).

When a finite-size sample is attached to two semi-infinite ideal leads, the condition (5) is sufficient to show that [27]

$$G = -\int_{S_1}\int_{S_2} \mathrm{d}\boldsymbol{S}_1 \cdot \underline{\sigma}(\boldsymbol{r}, \boldsymbol{r}') \cdot \mathrm{d}\boldsymbol{S}_2, \tag{6}$$

by using the divergence theorem to push the integration from the bulk onto the boundary surface[2] going through the leads and around the disordered sample (the integration over this

[2] Technical subtleties (like proper order of non-commuting limits) in finding zero and non-zero surface terms in the microscopic formulation of linear transport in open systems are detailed in [27].

insulating boundary obviously gives zero contribution because no current flows out of it). The surface integration in the two-probe conductance formula (6) is over surfaces S_1 and S_2 separating the leads from the disordered sample. The vectors $\mathrm{d}\boldsymbol{S}_1$ and $\mathrm{d}\boldsymbol{S}_2$ are normal to the cross-sections of the leads, and are directed outwards from the region encompassed by the overall surface (composed of S_1, S_2 and insulating boundaries of the sample). It is assumed that voltage in one of the leads is zero, e.g., $\mu_L = 0$ and $\mu_R = eV$. The meaning of current conservation and expression (6) are quite transparent: current I at a given cross-section depends only on the voltages in the leads (in experiment one either fixes this voltage by using a voltage source, or fixes the current by using a current source) and not on the precise electric field configurations. The formula (6) can be generalized [27] to arbitrary multiprobe geometry, while the volume-averaged conductance (4) is meaningful only for the two-probe measurement. The expression (6) is valid even in the presence of interactions, where many-body effects can be introduced using Kubo formalism to get $\underline{\sigma}(\boldsymbol{r}, \boldsymbol{r}')$ microscopically. However, this route is tractable and useful especially in the case of non-interacting quasiparticle systems. When a sample is attached to ideal leads (see below), this establishes rigorous equivalence [27] between two different linear response formulations—Kubo and Landauer–Büttiker [11] (to work out the proof, S_1 and S_2 should be placed far enough into the leads that all evanescent modes from the sample have died out and do not contribute to the conductance [4]). In the scattering approach to transport, pioneered by Landauer through heuristic and subtle arguments, the conductance of a non-interacting system is then expressed in terms of the probabilities of transmission between different quantized transverse propagating modes defined by the leads as asymptotic scattering states (see equation (28)).

Although the Boltzmann formalism can provide a semiclassical expression for NLCT (which is non-local on the scale of the sample size because of the classical requirement of current conservation [32]), the standard quantum route to it is the Kubo linear response theory (KLRT). Linear response theory gives a full quantum description of transport (i.e., it includes quantum interference effects in the motion of electrons[3]) in non-equilibrium systems that are still close enough to equilibrium for vanishingly small applied external electric field[4]. Therefore, the formulae above involve the equilibrium expectation values of the corresponding quantum-mechanical operators, in accordance with the fluctuation-dissipation theorem underlying KLRT (e.g., it is assumed that $\boldsymbol{j}(\boldsymbol{r})$ is the expectation value of the current density operator in the quantum formalism). While the current is a response to the total electric field (*external + induced*), the NLCT is obtained as a response to the external field only [33, 34] because the current induced by the external field is already linear in the field. Therefore, in the linear response one does not need the corrections due to induced non-equilibrium charges (also electron–electron interactions should be treated in equilibrium, e.g. through renormalized parameters of the Landau quasiparticles and the self-consistent screening effect on the impurity scattering).

Since Kubo NLCT is not an experimentally measurable quantity, the macroscopic conductivity σ is obtained by volume averaging NLCT through equation (4) where $\sigma = GL/S$ for a cubic sample of length L and cross-section S (the limit $\Omega = LS \to \infty$ is assumed, while keeping the impurity concentration finite). This usually implies homogeneous $\boldsymbol{E}(\boldsymbol{r})$ factors—which is justified by the fact that Kubo expression for NLCT is divergenceless (as can be easily

[3] For a long time it seemed that these rigorous (quantum) formulations of transport were merely serving to justify the intuitively appealing Boltzmann approach. The new viewpoint came with the first explicit calculation of quantum corrections like weak localization [42]—a quantum interference effect which generates a negative correction term to the Boltzmann result, and is responsible at low temperatures for all of the temperature and magnetic field dependence.

[4] The relation of 'vanishing' eV to the other relevant energy scales in the linear (quantum) transport regime is reviewed in [18].

proven [31] from its current–current correlation form [23]), i.e., satisfying equation (5). Thus, the volume-averaged conductivity σ relates the spatially averaged current $\boldsymbol{j} = \int \mathrm{d}\boldsymbol{r}\, \boldsymbol{j}(\boldsymbol{r})/\Omega$ to the spatially averaged electric field:

$$\boldsymbol{j} = \sigma \boldsymbol{E}. \tag{7}$$

For a non-interacting system of fermions this leads to a Kubo formula in the exact single-particle state representation (KFESR):

$$\sigma_{xx} = \frac{2\pi\hbar e^2}{\Omega} \sum_{\alpha,\alpha'} |\langle\alpha|\hat{v}_x|\alpha'\rangle|^2 \delta(E_\alpha - E_F)\delta(E_{\alpha'} - E_F), \tag{8}$$

where the factor of two for spin degeneracy will be explicit in all formulae. The delta functions in equation (8) emphasize that conductivity is a Fermi surface (E_F is the Fermi energy) property at low temperatures ($T \to 0 \Rightarrow -\partial f(E)/\partial E \simeq \delta(E_F - E)$, $f(E)$ being the Fermi–Dirac distribution function). Here $\hat{v}_x$ is the x-component of the velocity operator and $|\alpha\rangle$ are eigenstates of a single-particle Hamiltonian, $\hat{H}|\alpha\rangle = E_\alpha|\alpha\rangle$. The velocity operator $\hat{\boldsymbol{v}}$ is determined through the equation of motion for the position operator $\hat{\boldsymbol{r}}$:

$$\mathrm{i}\hbar\hat{\boldsymbol{v}} = \mathrm{i}\hbar\frac{\mathrm{d}\hat{\boldsymbol{r}}}{\mathrm{d}t} = [\hat{\boldsymbol{r}}, \hat{H}], \tag{9}$$

where $\hat{H}$ is the Hamiltonian before the application of the external electric field (in the spirit of FDT).

In the general case, conductivity is a tensor, but since symmetries are restored after disorder averaging, one can use $\sigma = (\sigma_{xx}+\sigma_{yy}+\sigma_{zz})/3$ as the scalar conductivity. This is valid only in the case of a homogeneously disordered sample. For example, in our metal junction or multilayers, σ_{xx} is different from σ_{yy} and σ_{zz}. To get the conductivity (as an intensive quantity) in KLRT, the thermodynamic limit Ω is always understood (no stationary regime can be reached in a system which is neither infinite nor coupled to some thermostat). In the disordered electron physics, this also bypasses the ambiguity of conductivity which scales [35] with the length of the system (although scaling is unimportant [22] in the metallic regime $G \gg G_Q$). Nonetheless, the computation of transport properties from exact single-particle eigenstates, obtained by the numerical diagonalization of Hamiltonian of a finite-size system, has been frequently employed throughout the history of disordered electron physics [25]. In fact, it is still the standard method for computing the conductivity of many-body systems where small clusters of some lattice fermion Hamiltonian are diagonalized [36], or in the calculations of high-temperature resistivity which treat phonons semiclassically by diagonalizing a single-particle Hamiltonian with frozen random atomic displacements [37]. However, direct application of the formula (8) leads to trouble, since eigenvalues are discrete when the sample is finite and isolated. Strictly speaking, the conductivity is then a sum of delta functions, and to obtain finite conductivity they have to be broadened into functions having a finite width larger than the level spacing. Thus, there are two numerical tricks which can be used to 'circumvent' this problem: (i) one can start from the Kubo formula for the frequency-dependent conductivity:

$$\sigma_{xx}(\omega) = \frac{2\pi\hbar e^2}{\Omega} \sum_{\alpha,\alpha'} |\langle\alpha|\hat{v}_x|\alpha'\rangle|^2 \frac{f(E_\alpha) - f(E_{\alpha'})}{\hbar\omega} \delta(E_\alpha - E_{\alpha'} - \hbar\omega), \tag{10}$$

average the result over finite ω-values, and finally extrapolate [38] to the static limit $\omega \to 0$; (ii) the delta functions in equation (8) can be broadened into a Lorentzian

$$\delta(x) \to \bar{\delta}(x) = \frac{1}{\pi} \frac{(\eta/2)^2}{x^2 + (\eta/2)^2}, \tag{11}$$

where η is the full width at half-maximum of the Lorentzian. I find that the two methods produce similar results. The calculations presented below use the broadened delta function $\bar{\delta}(x)$ in the formula for static Kubo conductivity.

The Green operator of a non-interacting Hamiltonian (with specified boundary conditions):

$$\hat{G}^{r,a} = [E - \hat{H} \pm \mathrm{i}\eta]^{-1} \tag{12}$$

contains the same information as is encoded in the single-particle wavefunction. Therefore, using the expansion of the single-particle Green operator $\hat{G}^{r,a} = \sum_\alpha |\alpha\rangle\langle\alpha|/(E - E_\alpha \pm \mathrm{i}\eta)$ in terms of exact eigenstates, the Kubo formula for the macroscopic (volume-averaged) longitudinal conductivity can be recast into the following expression [39]:

$$\sigma_{xx} = \frac{2\pi e^2\hbar}{\Omega} \mathrm{Tr}[\hat{v}_x \delta(E - \hat{H}) \hat{v}_x \delta(E - \hat{H})], \tag{13a}$$

$$\delta(E - \hat{H}) = -\frac{1}{\pi} \mathrm{Im}\, \hat{G} = \frac{1}{2\mathrm{i}}(\hat{G}^r - \hat{G}^a). \tag{13b}$$

When employing this formula one faces the same problem as in the KFESR—in order to define [40] the retarded (r) or advanced (a) Green function, a small parameter $\eta \to 0^+$ requires numerical handling [41] analogous to that (11) involved in the KFESR (8). However, it is possible to derive another, 'mesoscopic Kubo formula' for the finite-size sample attached to two semi-infinite clean leads [16, 27]. This formula represent a fully quantum-mechanical expression for the zero-temperature conductance:

$$G_{xx} = \frac{4e^2}{h} \frac{1}{L_x^2} \mathrm{Tr}(\hbar \hat{v}_x \,\mathrm{Im}\, \hat{G} \hbar \hat{v}_x \,\mathrm{Im}\, \hat{G}), \tag{14}$$

which, being measurable, is the only meaningful quantity to discuss in mesoscopics (the alternative is to introduce conductivity as the NLCT). That is, for quantum-coherent samples ($L > L_\phi$), local description of transport in terms of conductivity breaks down because of the non-local correction (e.g., weak localization [42]) induced on the scale of $L_\phi \gg \ell$, which is much larger than the elastic mean free path. Thus, a mesoscopic sample has to be treated as a single coherent unit ('giant molecule'), so its conductance cannot be interpreted as a combination $G = \sigma A/L$ of the conductances of its parts (i.e., such description becomes applicable only at high enough temperatures). Although the formula (14) apparently looks like equation (13), the crucial difference is that the following Green operator is plugged in there instead:

$$\hat{G}^{r,a} = [E - \hat{H} - \hat{\Sigma}^{r,a}]^{-1}. \tag{15}$$

This change is not innocuous: $\hat{G}^r$ ($\hat{G}^a = [\hat{G}^r]^\dagger$, $\hat{\Sigma}^a = [\hat{\Sigma}^r]^\dagger$) has acquired a self-energy term from the 'interaction' with the leads [18]. This looks like the self-energy term in the many-body Green functions, but this one is exactly calculable, as shown below. Thus, the leads enforce new boundary conditions. Since $\hat{\Sigma}^r(E)$ contains an imaginary part when energy E belongs to the band of a lead, no small parameter η is needed to define the retarded or advanced Green operator.

The lattice model of a two-probe measuring geometry, to be used in the subsequent sections for evaluation of equation (14), is shown in figure 1. The three-dimensional (3D) nanocrystal ('sample') is placed between two ideal (disorder-free) semi-infinite 'leads' which are connected smoothly to macroscopic reservoirs at infinity. The electrochemical potential difference $eV = \mu_L - \mu_R$, which drives the current [43], is measured between the reservoirs. It is assumed that reservoirs inject thermalized electrons at electrochemical potential μ_L (from the left) or μ_R (from the right) into the system. All inelastic scattering occurs in the reservoirs, which therefore ensure steady-state transport in the central region. Semi-infinite leads [44]

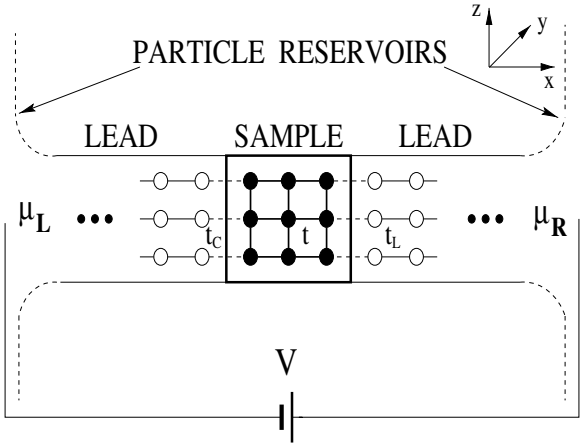

Figure 1. A two-dimensional version of the actual 3D model used here for a two-probe measuring geometry. Each site hosts a single s orbital which hops to six (or fewer for surface atoms) nearest neighbours. The hopping matrix element is t (within the sample), $t_{\rm L}$ (within the leads), and $t_{\rm C}$ (coupling of the sample to the leads). The leads are semi-infinite and connected smoothly at $\pm\infty$ to macroscopic reservoirs biased by the chemical potential difference $\mu_L - \mu_R = eV$.

are a convenient means to take into account electrons entering or leaving the phase-coherent sample (i.e., the effective Hamiltonian of an open system, $\hat{H} + \hat{\Sigma}^r$ in equation (15), is non-Hermitian). This makes it possible to bypass explicit modelling of the thermodynamics of perfect (i.e., unaffected by the flow of current) macroscopic reservoirs which are introduced heuristically in the scattering approach (for a different interpretation of the role of perfectly conducting leads in the derivation of the Kubo formula for a finite-size system, see [45]). The leads have the same cross-section as the sample, which eliminates scattering induced by the wide-to-narrow geometry at the sample–lead interface [46]. The whole system is described by the following Hamiltonian with nearest-neighbour hopping integrals t_{mn}:

$$\hat{H} = \sum_{m} \varepsilon_m |\boldsymbol{m}\rangle\langle\boldsymbol{m}| + \sum_{\langle m,n\rangle} t_{mn} |\boldsymbol{m}\rangle\langle\boldsymbol{n}|. \tag{16}$$

where $\langle \boldsymbol{r}|\boldsymbol{m}\rangle$ is the s orbital $\psi(\boldsymbol{r}-\boldsymbol{m})$ located on site $\boldsymbol{m}$. The site representation, defined by the basis states $|\boldsymbol{m}\rangle$, can be interpreted either as a tight-binding description of electronic states or as discretization of the corresponding single-particle Schrödinger equation. The sample is the central section with $N \times N_y \times N_z$ sites. The hopping in the sample sets the unit of energy $t_{mn} = t$. The disorder will be introduced by taking ε_m to be a random variable. The leads are clean ($\varepsilon_m = 0$) but, in general, have different hopping integrals $t_{mn} = t_{\rm L} \neq t$. Finally, the hopping which couples the sample to the leads is $t_{mn} = t_{\rm C}$. Hard-wall boundary conditions are set in the $\hat{y}$- and $\hat{z}$-directions. The different hopping integrals introduced here are necessary when studying disordered samples to get the conductance at Fermi energies throughout the whole band extended (compared to the clean case) by disorder, i.e., in such calculations one has to set $t_{\rm L} > t$.

In site representation, the Green operator $\hat{G}^{r,a}$ becomes a Green function matrix $\hat{G}^{r,a}(\boldsymbol{n},\boldsymbol{m}) = \langle \boldsymbol{n}|\hat{G}^{r,a}|\boldsymbol{m}\rangle$. The self-energy $\hat{\Sigma}^r = \hat{\Sigma}^r_L + \hat{\Sigma}^r_R$ 'measures' the coupling of the sample to the leads. This causes the broadening of initially discrete levels and, thus, the finite lifetime of the electron in the sample. Since an electron which leaves the sample does not return phase coherently, the dephasing length is by definition $L_\phi = L_x$. Each lead generates its self-energy term which has non-zero matrix elements only on the edge layers of the sample

which are adjacent to the leads. They are defined as

$$\hat{\Sigma}^r_{L,R}(\boldsymbol{n},\boldsymbol{m}) = t_{\mathrm{C}}^2 \hat{g}^r_{L,R}(\boldsymbol{n}_S,\boldsymbol{m}_S), \tag{17}$$

with $\hat{g}^r_{L,R}(\boldsymbol{n}_S,\boldsymbol{m}_S)$ being the surface Green function of a bare semi-infinite lead between the sites $\boldsymbol{n}_S$ and $\boldsymbol{m}_S$ in the end atomic layer of the lead [18] (adjacent to the corresponding sites $\boldsymbol{n}$ and $\boldsymbol{m}$ inside the conductor). I provide here an explicit expression for these self-energy terms in the most general case, when hopping integrals $t \neq t_{\mathrm{C}} \neq t_{\mathrm{L}}$ are different in different parts of the set-up, in figure 1:

$$\hat{\Sigma}^r_{L,R}(\boldsymbol{n},\boldsymbol{m}) = \frac{2}{N_y+1}\frac{2}{N_z+1}\sum_{k_y,k_z} \sin(k_y n_y a)\sin(k_z n_z a)\hat{\Sigma}^r(k_y,k_z)\sin(k_y m_y a)\sin(k_z m_z a). \tag{18}$$

This expression is obtained by expanding the surface Green function $\hat{g}^r_{L,R}(\boldsymbol{n}_S,\boldsymbol{m}_S)$ in terms of exact eigenstates of the Hamiltonian of a semi-infinite lead, which satisfy particular hard-wall transverse boundary conditions. Here $(\boldsymbol{n},\boldsymbol{m})$ is the pair of sites on the surfaces inside the sample which are adjacent to the leads L or R, in accordance with (17). Since electrons are confined in the y- and z-directions, electronic states in the lead have transverse wavefunctions which are labelled by the discrete quantum numbers. They define subbands and corresponding conducting 'channels' (i.e., transverse propagating modes as the product of transverse wavefunctions and Bloch waves in the x-direction, $\langle \boldsymbol{m}|k_y,k_z\rangle \otimes |k_x\rangle$), which represent a basis of scattering states for the scattering matrix of the disordered region, as envisaged in the Landauer picture of quantum transport. The self-energy $\hat{\Sigma}^r(k_y,k_z)$ of the channel (k_y,k_z) is given by

$$\hat{\Sigma}^r(k_y,k_z) = \frac{t_{\mathrm{C}}^2}{2t_{\mathrm{L}}^2}\left(E_\Sigma - \mathrm{i}\sqrt{4t_{\mathrm{L}}^2 - E_\Sigma^2}\right), \tag{19}$$

for $|E_\Sigma| < 2t_{\mathrm{L}}$. I use the shorthand notation $E_\Sigma = E - \varepsilon(k_y,k_z)$, where $\varepsilon(k_y,k_z) = 2t_{\mathrm{L}}[\cos(k_y a)+\cos(k_z a)]$ is the energy of quantized transverse levels in the lead. In the opposite case $|E_\Sigma| > 2t_{\mathrm{L}}$ we get

$$\hat{\Sigma}^r(k_y,k_z) = \frac{t_{\mathrm{C}}^2}{2t_{\mathrm{L}}^2}\left(E_\Sigma - \mathrm{sgn}E_\Sigma\sqrt{E_\Sigma^2 - 4t_{\mathrm{L}}^2}\right). \tag{20}$$

When the level spacing of the subbands is much smaller than E_F, the number of channels at E_F is large and the finite-size model can describe a metal. The possibility of evaluating these self-energies exactly allows us to avoid the inversion of an infinite matrix which would formally give the Green function for the whole system [18] in figure 1. The real-space Green function technique described here, pioneered by Caroli *et al* [15] long before the official inception of mesoscopic physics, treats an infinite system with a continuous spectrum by evaluating only the Green function between the states inside the sample. This offers an alternative to handling a finite-size sample through periodic boundary conditions, whose discrete spectrum prevents a direct evaluation of the Kubo formulae (8) and (13). In general, the technical advantage of Green function techniques is that they can be used even when well-defined asymptotic conducting channels in the scattering approach to quantum transport are hard to define (e.g., this is the case when leads have complicated shape [47], making it hard to get explicitly the exact asymptotic eigenstates and their eigenspectrum).

The mesoscopic Kubo formula can be evaluated at any (continuous) Fermi energy. At first sight, it seems like that this leads to a much greater computational complexity than in the case of KFESR because of the need to find inverse matrix in equation (15) at each chosen energy, and then perform the trace over the site states $\mathrm{Tr}(\ldots) = \sum_{\boldsymbol{m}}\langle \boldsymbol{m}|(\ldots)|\boldsymbol{m}\rangle$. On the

other hand, in the KFESR one needs to diagonalize the Hamiltonian only once and then use the eigenstates obtained to compute matrix elements of the velocity operator in the eigenbasis. However, this is only an apparent difficulty once the conservation of current is invoked. Since all Kubo formulae for conductance stem from equation (4), one has to assume (or choose) some electric field factors therein. Current conservation, i.e., the fact that I has to be the same on each cross-section, means that the conductance is independent of this choice. The minimal space for tracing, when the system is described by a TBH in equation (16), is obtained by taking both factors $\boldsymbol{E}(\boldsymbol{r})$ and $\boldsymbol{E}(\boldsymbol{r}')$ to be non-zero only on two adjacent planes of the lattice. That is, the expectation value of the velocity operator (9) in the site representation is non-zero only between the states residing on adjacent planes:

$$\langle \boldsymbol{m}|\hat{v}_x|\boldsymbol{n}\rangle = \frac{\mathrm{i}}{\hbar} t_{mn}(m_x - n_x), \tag{21}$$

for a TBH (16) with nearest-neighbour hopping. The final result is then to be divided by a^2 (instead of L_x^2 in equation (14)).

Thus, only a block matrix $2N_zN_y \times 2N_zN_y$ of the Green function for the whole sample has to be computed explicitly (e.g., those elements which connect the first two planes of the sample in figure 1). Because $[E - \hat{H} - \hat{\Sigma}^r]$ is a band-diagonal matrix of bandwidth $2N_yN_z + 1$, one can substantially shorten the time needed to compute this block of the Green function (15) by finding the LU decomposition of a band-diagonal matrix, followed by forward–backward substitution for each Green function element needed [48]. This requires a similar number of operations [49] to the more familiar recursive Green function technique [44].

3. Transport through dirty metal junctions

This section studies the static DC transport properties of a metal junction composed of two disordered conductors with different kind of disorder introduced on each side of the contact interface. Both conductors are modelled as a disordered binary alloy (i.e., composed of two types of atom, A and B) using the TBH of equation (16). The quenched disorder is simulated by taking the random on-site potential such that ε_m is either ε_A or ε_B, with equal probability. Specifically, I take the lattice as $18 \times 8 \times 10$ on each side of the junction and for the binary disorder: $\varepsilon_A = -4$, $\varepsilon_B = 0$ on the left; and $\varepsilon_A = 4$ and $\varepsilon_B = 0$ on the right. Thus, the junction has naturally a rough interface [14] because of the random positions of three different types of atom around the plane in the middle of the junction.

We commence with a description of the junction, as well as the homogeneous samples used as a reference, in terms of traditional Kubo theory based on the KFESR (8). Although [44] stated as one of the motivations for undertaking the rigorous derivation of the Landauer two-probe formula from KLRT that traditional use of the Kubo formula [25] was numerically demanding, today's computers are much more powerful, and it is of interest to compare this method to a modern [16] mesoscopic use of the Kubo formula. Kubo theory permits discussion of the diffusivity D_α of an eigenstate $|\alpha\rangle$. This quantity is extracted directly from the KFESR for a Fermi gas of non-interacting quasiparticles:

$$\sigma = \frac{1}{\rho} = \frac{e^2}{\Omega} \sum_\alpha \left(-\frac{\partial f}{\partial E_\alpha} \right) D_\alpha = e^2 N(E_F) \bar{D}. \tag{22}$$

Thus, the quantum diffusivity is given explicitly by the following expression:

$$D_\alpha^x = \pi\hbar \sum_{\alpha'} |\langle \alpha|\hat{v}_x|\alpha'\rangle|^2 \delta(E_\alpha - E_{\alpha'}). \tag{23}$$

In the semiclassical regime, $D_\alpha \to D_k = v_k \ell_k/3$. However, D_α can also be used to characterize transport in strong disorder causing non-perturbative quantum effects, which

invalidate semiclassical concepts (e.g. putative mean free path l in this transport regime, extracted from the semiclassical Boltzmann equation, would be smaller than the lattice spacing [21].

To simplify the calculations, I compute the quantum diffusivity $\langle D_x(E_F)\rangle$ averaged over the disorder ($\langle\cdots\rangle$ denotes averaging over an impurity ensemble), as well as over a small energy interval. This is additional transport information, obviously related to conductivity (22), which is not usually seen in the literature on disordered electron physics [50]. It has been exploited in the transport physics of glasses (e.g., to study the thermal conductivity in amorphous silicon [38]). The width η of the Lorentzian $\bar{\delta}(E_\alpha - E_{\alpha'})$ in (23) is chosen as some multiple of the local average level spacing $\Delta(E_\alpha)$ in a small energy interval around the eigenenergy E_α. The method of computing $\langle D_x(E_F)\rangle$ is as follows: a set of eigenstates (the number of eigenstates is equal to the number of lattice sites $N_s = N \times N_y \times N_z$) is obtained by numerical diagonalization; $\mapsto$ for each eigenstate I compute D_α^x, where the summation is over all states $|\alpha'\rangle$ 'picked' by the Lorentzian $\bar{\delta}(E_\alpha - E'_\alpha)$ (centred on E_α) in an energy interval of 3η around E_α; $\mapsto$ finally, I average the diffusivities over the disorder and energy interval defined by a bin of size $\Delta E = 0.0225$. The efficient way of calculating quantum-mechanical average values of some operator, such as $\langle\alpha|\hat{v}_x|\alpha'\rangle$ appearing in the definition of eigenstate diffusivity (23), is to multiply three matrices $\hat{\alpha}^\dagger\hat{v}_x\hat{\alpha}$, where $\hat{\alpha}$ is a matrix containing eigenvectors $|\alpha\rangle$ as columns, and then take the modulus squared of each matrix element in such a product. The number of operations in the naive calculation of the expectation values of the operator, where each of them is calculated separately, scales as $\sim N_s^4$, while in the method presented above it scales as $\sim N_s^3$ ($N_s \times N_s$ is the dimension of the operator matrix). This procedure becomes a natural choice once we understand that it actually transforms the matrix of the operator $\hat{v}_x$ from the defining (site) representation into the representation of eigenstates $|\alpha\rangle$. The end result of the calculation, the average diffusivity $\langle D_x\rangle$, is related to the conductivity through the Einstein relation

$$\sigma_{xx} = e^2 N(E_F)\langle D_x(E_F)\rangle. \tag{24}$$

Here $N(E_F)$ is the density of states (DOS) (for both spin components) evaluated at the Fermi level E_F.

I first calculate $\langle D_x(E_F)\rangle$ for the homogeneously disordered sample (with binary disorder $\varepsilon_A = -2$, $\varepsilon_B = 2$) modelled on an $18 \times 8 \times 10$ lattice, as shown in figure 2. To get insight into the microscopic features of the eigenstates used to evaluate the KFESR (a few eigenstates around each E_F determine the transport properties at E_F), this figure also plots the inverse participation ratio (IPR) [51]

$$I_2 = \Delta\left\langle \sum_{m,\alpha} |\Psi_\alpha(m)|^4 \delta(E - E_\alpha)\right\rangle, \tag{25}$$

averaged over disorder and energy [$\Psi_\alpha(m) = \langle m|\alpha\rangle$]. This is the simplest single-number measure of the degree of localization (i.e., the bigger the IPR, the more localized the state; e.g. IPR $= N_s$ corresponds to a completely localized state on one lattice site). The IPR can also be related to the average return probability [19] that a particle, initially launched in a state $|m\rangle$ localized on a lattice site m, will return to the same site after a very long time (which is determined by its diffusive properties encoded in D_α). The second calculation, shown in figure 3, is for the homogeneous sample described by the standard Anderson model where $\varepsilon_m \in [-W/2, W/2]$ is a uniform random variable. This results are to be compared to the reference calculation based on the mesoscopic Kubo formula.

Strictly speaking, the concept of 'eigenstate' does not apply to open systems. Such systems can be characterized by non-Hermitian Hamiltonians [18], which do not conserve

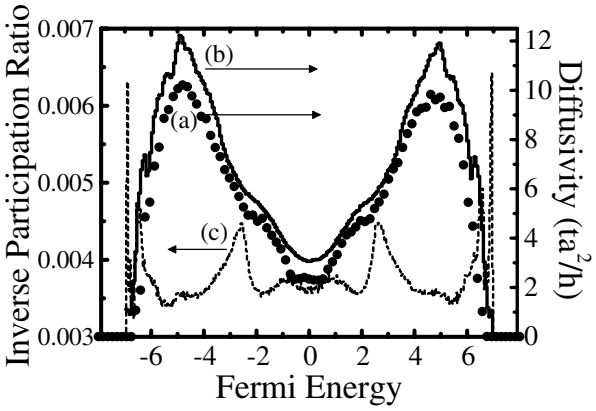

Figure 2. Diffusivity $\langle D_x(E_F)\rangle$ of a disordered binary alloy modelled by a TBH with quenched disorder ($\varepsilon_A = -2$ and $\varepsilon_B = 2$) on an $18 \times 8 \times 10$ lattice: (a) computed using the Kubo formula (14) in terms of the Green function for the sample with attached leads; (b) computed from the Kubo formula in the exact single-particle eigenstate representation (23), where the width of the Lorentzian-broadened delta function is $\eta = 25\Delta(E_F)$. Also plotted (c) is the IPR, defined in equation (25), which gives insight (i.e., degree of localization) into the structure of eigenstates used to evaluate the Kubo formula, equation (23). The disorder averaging is performed over 50 samples.

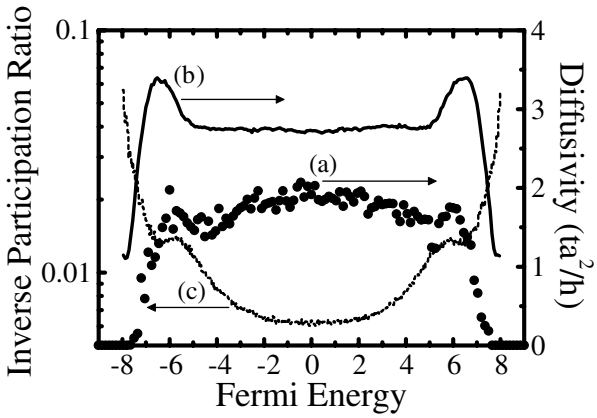

Figure 3. The result of the same computation of $\langle D_x(E_F)\rangle$ as in figure 2, but for a different type of disorder, a diagonal one of strength $W = 10$, introduced in the sample (the same labels apply to both figures).

total probability (cf section 2). This is a consequence of a simple physical fact that an electron stays for a finite time within the sample before escaping into the surrounding leads (i.e., initial discrete energy levels are broadened by the coupling to the leads). Nonetheless, we can still get [22] the DOS from the imaginary part of the Green function (15):

$$N(E_F) = \sum_m -\frac{1}{\pi} \operatorname{Im} \hat{G}^r(\boldsymbol{m}, \boldsymbol{m}; E_F). \tag{26}$$

That such a DOS of an open 3D system is indistinguishable from the one computed from the distribution of energy eigenvalues, $N(E_F) = (2/\Omega)\langle\sum_\alpha \delta(E_F - E_\alpha)\rangle$, is shown in figure 4. This is in spite of the fact that leads strongly perturb the edges of the system, which is clearly exhibited only for the smallest lattice in figure 4. Thus, the average diffusivity $\langle D_x(E_F)\rangle$ can

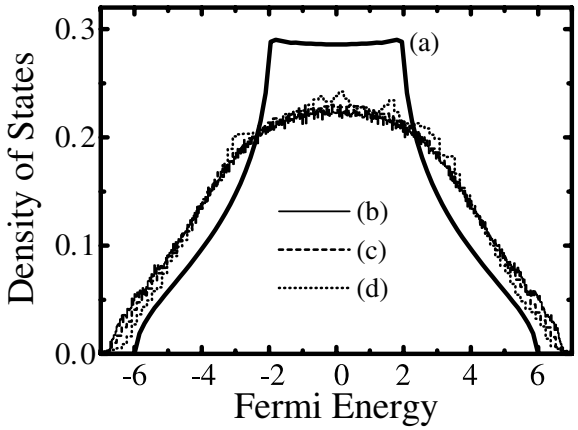

Figure 4. The DOS of: (a) clean metal ($W = 0$); (b) dirty metal ($W = 6$ on a $15 \times 15 \times 15$ lattice averaged over 50 disorder configurations), obtained as $N(E) = (2/\Omega)\sum_\alpha \delta(E - E_\alpha)$ from the exact eigenspectrum E_α of a closed sample Hamiltonian; (c) dirty metal ($W = 6$ on a $10 \times 10 \times 10$ lattice averaged over 50 disorder configurations), obtained from the imaginary part, equation (26), of the Green function (15) of an open sample. (d) is computed in the same way as (c) except that a smaller lattice, $4 \times 4 \times 4$, is used.

be computed in a straightforward manner from the Einstein relation (24) where conductivity is formally expressed in terms of the disorder-averaged conductance $\sigma_{xx} = \langle G_{xx} \rangle L_x/S$ given by the mesoscopic Kubo formula.

In both calculations for the homogeneous samples it appears that the discrepancy between the Kubo formula in the single-particle representation (8) and the exact method, based on the formula (14) for the *sample + lead* system, is only numerical. In fact, the difference is very small in the disordered binary alloy and a bit larger in the Anderson model with continuous disorder. It originates from the ambiguity in using the width η of the broadened delta function. That is, non-zero η effectively introduces inelastic scattering as an uncorrelated random event [41]. The increase of the diffusivity close to the band edges of the diagonally disordered Anderson model (cf figure 3) was seen a long time ago in direct simulations of the wavefunction diffusion performed in the early days of localization theory [50].

The same analysis is repeated for a junction (introduced at the beginning of this section) which is composed of two different disordered binary alloys on each side. The result is shown in figure 5. Large fluctuations of the diffusivity (i.e., quantum conductance G from which the diffusivity is computed at specific E_F) are caused by the conductance being of the order of $2e^2/h$ (figure 8). Such fluctuations are less obvious in the result based on the KFESR because of the extra averaging over energy provided by the Lorentzian-broadened delta function. Here the discrepancy between the two different methods is not only quantitative, but the KFESR (8) shows non-zero diffusivity (and thereby conductivity, since the global DOS is non-zero throughout the band) at Fermi energies at which there are no states on one side of the junction which can carry the current[5]. The result persists even when the width η of the Lorentzian-broadened delta function is decreased. Therefore, it is not an artefact of the numerical trick used to evaluate the KFESR. The states which have non-zero amplitude throughout the junction cease to exist at $|E_b| \sim 4.7$, which is seen by inspecting the local

[5] Intricacies in the application of the Kubo formula to finite-size samples, 'extended' through periodic boundary conditions, were discovered also in some other condensed matter problems, e.g. in the conduction in the 1D Hubbard model, see [52].

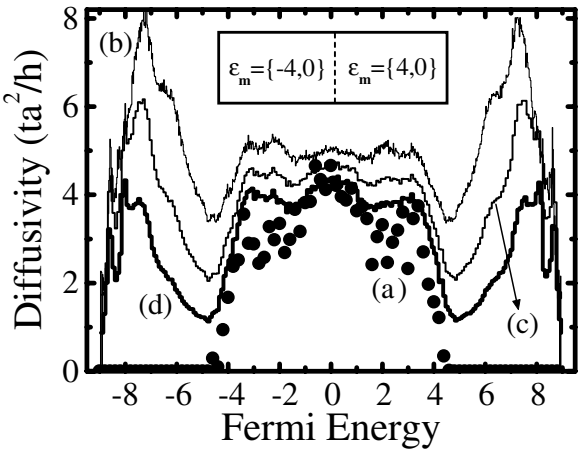

Figure 5. Diffusivity $\langle D_x(E_F)\rangle$ for a metal junction composed of two disordered binary alloys (modelled by a TBH on a $36 \times 8 \times 10$ lattice): (a) computed using the Kubo formula (14) in terms of the Green function for the sample with attached leads; and computed from the Kubo formula in the exact single-particle eigenstate representation (23), where the width of the Lorentzian-broadened delta function is (b) $\eta = 25\Delta(E_F)$, (c) $\eta = 10\Delta(E_F)$, and (d) $\eta = 5\Delta(E_F)$. Disorder averaging is performed over 50 different samples.

density of states (LDOS), integrated over y- and z-coordinates:

$$\rho(m_x, E) = \sum_{m_y,m_z} \rho(\boldsymbol{m}, E) = \sum_{m_y,m_z} \sum_{\alpha} |\Psi_\alpha(\boldsymbol{m})|^2 \delta(E - E_\alpha). \tag{27}$$

Such 'planar LDOS' along the x-axis is plotted in figure 6. It changes abruptly when going from one side of the junction to the other side (except for the small tails near the interface). On the other hand, figure 5 explicitly demonstrates that the Kubo formula (14) for an open finite-size sample plugged between ideal semi-infinite leads correctly describes this junction. That is, the diffusivity vanishes at the same point at which the LDOS goes to zero. It should be emphasized that once the leads are attached, two new interfaces (lead–sample) in the problem arise. The Landauer–Büttiker scattering approach to transport intrinsically takes care of these boundaries by considering a realistic finite-size system where electrons can leave or enter through some surfaces into the rest of the circuit represented by the leads [43, 52]. Thus, mesoscopic developments have clarified the way to properly apply the Kubo formulism to finite-size samples (which is ultimately related to the eternal puzzle of the origins of dissipation in conservative systems, technically the only ones appearing in the Kubo analysis) [53]. This in turn has justified heuristic arguments of Landauer on a rigorous basis [27, 44].

The conductance of an infinite (*sample + leads*) system will go to zero at the band edge of a clean lead $|E_b| = 6t$ if we use the same hopping parameter in the lead $t_L = t$ as in the disordered sample. This stems from the fact that are no states in the leads which can carry the current for Fermi energies $|E_F| > 6t$ outside of the clean TBH band. Technically, the self-energy $\hat{\Sigma}^r$ is real at these energies, which leads to Im $\hat{G}$ in (14) being zero. Thus, the conductance of the whole band of the disordered sample cannot be computed unless we increase t_L in the leads. This is illustrated in figure 7 for the homogeneous sample described by the Anderson model where the band edge of the disordered sample $|E_b| > 6t$ lies outside of the clean metal band defined by crystal symmetry. Thus, a natural question arises when using $t_L, t_C \neq t$: how sensitive is the conductance to the properties of leads or the sample–lead coupling? This problem resembles the quantum measurement problem because semi-infinite leads can also be viewed as a macroscopic apparatus necessary for measurement [28, 55].

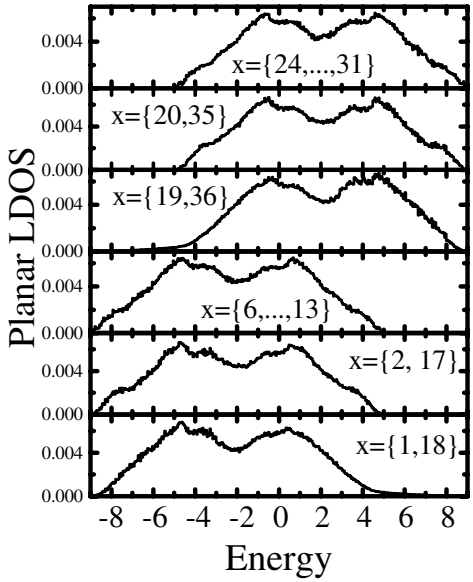

Figure 6. The LDOS integrated over the y- and z-coordinates inside the metal junction studied in figure 5. This 'planar LDOS' $\rho(m_x, E)$ is computed from the exact eigenstates of the TBH using equation (27). The result is plotted after $\rho(m_x, E)$ is averaged over several planes along the x-axis (the planes used in this procedure are given on each panel).

This is further stressed in multiprobe geometries [18] where extra leads are introduced to measure the voltages along the sample (besides the two leads, used here, through which the current is fed). The measured conductance is then a property of both the sample and the measurement geometry, which is one of the reasons for mesoscopic physics employing only sample- and measurement-geometry-specific quantities, such as quantum conductance, instead of intensive quantities, such as conductivity [33]. From a transport point of view, it is clear that lead–sample interfaces introduce extra scattering for different effective masses or Fermi velocities in the sample and the lead. Thus, the *exactness* of the conductance calculated here is, in fact, a feature of the whole *sample + leads* set-up in figure 1 (that is akin to any kind of measurement in quantum mechanics), and it is important to confirm that general conclusions about the relationship between different Kubo formulae do not depend on particular values of the chosen parameters for the leads.

It is understood [54] that if the broadening of the energy levels due to the coupling to semi-infinite leads is greater than the Thouless energy $E_{\mathrm{Th}} \simeq \hbar\mathcal{D}/L^2$, ($\mathcal{D}$ is the diffusion constant, i.e. the average quantum diffusivity introduced in this section), then level discreteness of an isolated sample is unimportant and G will be independent of the properties of the leads. This limit corresponds to an 'intrinsic' (Thouless) conductance $G/G_Q = 2\pi E_{\mathrm{Th}}/\Delta$ (Δ is the mean level spacing) that is smaller than the conductance determined by the lead–sample contact [56]. It requires a sufficiently disordered sample [55] and leads of the same cross-section as that of the sample [56]. Thus, even though attaching the sample to the leads causes dramatic changes (the discrete spectrum is changed into a continuous one and new boundary conditions are introduced), the conductance is determined by the sample properties only, and dissipation in the reservoirs does not enter into the computational algorithm. This dependence is studied in figure 8 by looking at the conductance of our model junction as a function of the hopping in the leads t_{L} and the coupling t_{C}. The conductance is virtually independent of t_{L}, which is a

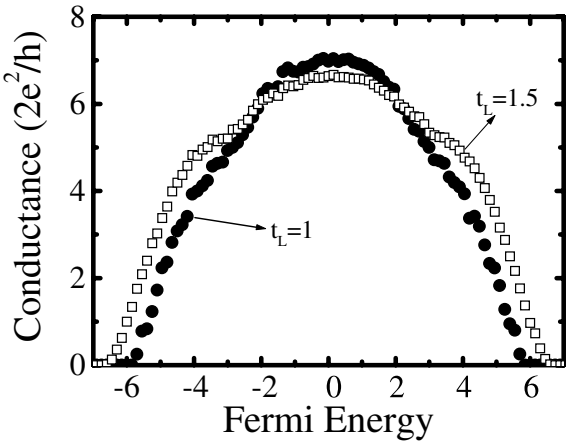

Figure 7. Two-probe conductance of a disordered conductor (averaged over 50 samples) modelled by the Anderson model with diagonal disorder $W = 6$ on a simple cubic lattice 10^3. The computation is done using the mesoscopic Kubo formula (14) for the finite sample attached to two semi-infinite leads characterized by two different values of the hopping integral t_L. Note that the conductance vanishes at $|E| = 6t$ (band edge in a clean sample) when $t_L = t$.

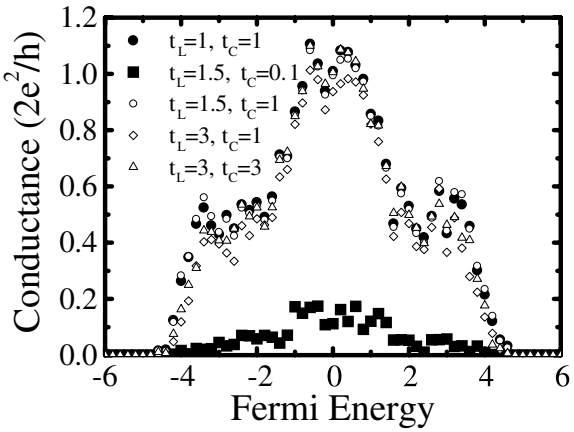

Figure 8. Two-probe conductance (averaged over 50 samples) of the same dirty metallic junction sample as in figure 5, but attached to two semi-infinite ideal leads with several different hopping integrals t_L or lead–sample couplings t_C (the hopping integral in the sample sets the unit of energy $t = 1$). The computation is based on the mesoscopic Kubo formula equation (14).

consequence of the smallness of the disordered junction conductance (as discussed above). It goes down drastically with decrease of the coupling t_C (the same behaviour is anticipated when t_L is increased substantially because of the increased reflection at the lead–sample interface).

4. Transport through a strongly disordered interface

In this section we analyse quantum transport properties of a single dirty interface whose dimensionless conductance G/G_Q is much smaller than the number of conducting channels N_{ch} (i.e., much smaller than the conductance of a ballistic conductor of the same cross-section). For practical purposes, the interface can be defined as any scattering region whose thickness is

sufficiently shorter than [5] λ_F (in bulk conductors, $L \gg \lambda_F$). Here we look at a geometrical plane of atoms as a model of an interface in the strict sense. Furthermore, we look at the evolution of transport from a single dirty interface to a strongly disordered thin slab (i.e., 'thin Anderson insulators', since stacking together enough finite-size interfaces, with the disorder strength chosen here, would lead to a bulk Anderson insulator with exponentially small conductance). Such thin slabs are a more likely element in experimental circuits [20]. These problems are not only conceptual—namely, how to understand the difference between the transport in bulk conductors and interfaces—but also have been raised by the understanding of crucial effects that the interface scattering can have in the CPP transport experiments [57] on GMR magnetic multilayers (in GMR the added complication is spin-dependent interface resistance [58] which dominates the resistance and magnetoresistance for layer thicknesses that are not too large [59]).

The importance of interface scattering in many areas of metal and semiconductor physics has been realized in a plethora of research papers since the seminal work of Fuchs [7]. They are mainly concerned with the transport parallel to an impenetrable rough interface, while recently interest has also arisen in the transport normal to the interface (CPP geometry). Because the nature of the transport relaxation time in inhomogeneous systems is not well understood [4], the first step is to understand properties of a single interface before studying them as a part of some more complicated circuit such as those in section 5. For example, the properties of a single interface cannot be described in terms of the Boltzmann conductivity $\sigma_B = ne^2\tau/m$, i.e., using the elastic mean free path $\ell = v_F\tau$ (or transport mean free time τ) familiar from the bulk metallic conductors whose conductivity is dominated by the semiclassical effects.

Lacking enough experimental information, the simple theoretical models for the interface effects on electron propagation assume diffuse scattering at interdiffused atoms or interfacial roughness [60] (these free electron theories omit the complex electronic band structure of transition metals appearing in realistic GMR samples). Even a disorder-free interface can have a non-zero resistance, because of mismatch of the crystal potential and band structures [4]. Here we are interested only in generic properties of mesoscopic transport through interfaces that do not depend on material-specific details [5]. Therefore, the interface roughness is modelled here by the short-range random scattering potential [12] generated by the impurities located on the sites of a square lattice, $1 \times N_y \times N_z$, and with strong disorder $W_I = 30$ in the corresponding TBH equation (16). The bulk conductor composed of such interfaces (stacked in parallel and coupled with nearest-neighbour hopping t) is an Anderson insulator, because all states are localized already for [61] $W_c \simeq 16.5$. To compute the CPP transport properties using the mesoscopic Kubo formula (14), the interface is placed in our standard computational set-up between the two semi-infinite disorder-free leads. Thus, the conductance is computed for an atomic monolayer of a disordered material inside an infinite clean sample of finite cross-section shown in figure 1. Also computed is the conductance of a thin slab composed of two (i.e., a 3D conductor modelled on the $2 \times N_y \times N_z$ lattice) and three sheets ($3 \times N_y \times N_z$) of the same disordered material, as shown in figure 9. The microscopic origin of different terms contributing to the interface resistance was traced back to both specular and diffusive scattering in the plane (where diffusive scattering can even open additional channels for electron transport, thereby increasing the conductance) [4].

Following the discussion in section 3, the influence of the leads on the interface conductance is checked by using two different hopping integrals t_{L} (compare to figure 7). Here the analysis based on comparison of relevant energy scales does not work (i.e., one cannot use bulk material concepts, like E_{Th}). Plausibly, I find that leads affect the conductance of the interface much more than the conductance of a bulk disordered conductor (with a similar value of disorder-averaged conductance).

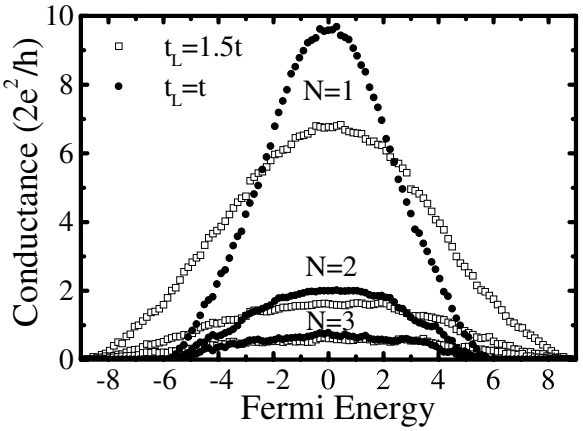

Figure 9. Conductance of a single dirty interface ($N = 1$) and thin slabs composed of two ($N = 2$) or three ($N = 3$) such interfaces (modelled by the Anderson model with diagonal disorder $W_I = 30$ on an $N \times 10 \times 10$ lattice). The calculation is performed using different values of the hopping parameter t_L in the attached leads, and the results are averaged over 200 realizations of disorder.

Mesoscopic transport methods give the possibility not only to compute the conductance, but also to use the picture of conducting channels and their quantum-mechanical transmission properties. From a pragmatic point of view, one does not need these fully quantum techniques to study the transport in macroscopic conductors which are usually dominated by semiclassical physics. Nevertheless, the study of the distribution of transmission probabilities, which requires phase-coherent transport, enhances our insight into the conduction processes in electronic systems. The diagonalization of a Hermitian matrix $\boldsymbol{t}\boldsymbol{t}^\dagger$, which defines the conductance through the Landauer formula:

$$G = \frac{2e^2}{h}\,\mathrm{Tr}(\boldsymbol{t}\boldsymbol{t}^\dagger) = \frac{2e^2}{h}\sum_{n=1}^{N_y N_z} T_n, \tag{28a}$$

$$\boldsymbol{t} = 2\sqrt{-\mathrm{Im}\,\hat{\Sigma}_L}\,\hat{G}^r_{1N}\sqrt{-\mathrm{Im}\,\hat{\Sigma}_R}, \tag{28b}$$

introduces a set of transmission eigenvalues $0 \leqslant T_n \leqslant 1$ for each realization of disorder. The incident flux concentrated in channel $|p\rangle$ will give the wavefunction in the opposite lead $\sum_q \boldsymbol{t}_{pq}|q\rangle$, where $\boldsymbol{t}$ is the transmission matrix. Here $\hat{G}^r_{1N}$ is the matrix block, which connects layers 1 and N of the sample, of the full retarded real-space Green function matrix (15). The distribution function of T_n is defined as

$$P(T) = \left\langle \sum_n \delta(T - T_n) \right\rangle. \tag{29}$$

Using $P(T)$, the disorder-averaged value of any quantity that can be written down in the form of linear statistics $a(T)$ is expressed as [62]

$$\langle A \rangle = \left\langle \sum_{n=1}^{N_{\mathrm{ch}}} a(T_n) \right\rangle = \int_0^1 \mathrm{d}T\, a(T) P(T). \tag{30}$$

For example, the conductance is described by a linear statistics $g(T) = T$. Contrary to naive expectations, stemming from comparison with Drude–Boltzmann conductance $G \simeq G_Q N_{\mathrm{ch}} \ell/L$, that the transmission of every channel is $T \simeq \ell/L$ in the metallic diffusive

($G_Q N_{\rm ch} \gg G \gg G_Q$) bulk conductor, it was shown by Dorokhov [63] that in a homogeneous multichannel wire geometry

$$P_{\rm D}(T) = \frac{G}{2G_Q}\frac{1}{T\sqrt{1-T}}, \qquad \cosh^{-2}\left(\frac{N_{\rm ch}}{g}\right) < T < 1. \tag{31}$$

The cut-off [5] at small T is such that $\int_0^1 {\rm d}T\, P(T) = N_{\rm ch}$ ensuring that averages of the first- and higher-order moments of T are not affected (with the proviso that $N_{\rm ch} \gg G/G_Q$). The Dorokhov distribution is universal—it depends only on the disorder-averaged conductance G and not on the details of disorder, dimension, shape of the sample, carrier density, spatial resistivity distribution, and other sample-specific properties [62]. Thus, $P(T)$ is a bimodal distribution function, meaning that: most of the T_n are either $T_n \simeq 0$ ('closed' channels) or $T_n \simeq 1$ ('open' channels). This has important consequences when calculating linear statistics other than the conductance, since we can get conductance (first moment of the distribution) without really knowing the details of $P(T)$ (e.g., the higher moments are probed in the case [62] of shot-noise power, and Andreev conductance of metal/superconductor interfaces).

The simple counting of the number of T_n in each bin across the interval [0, 1] allows us to obtain the distribution function $P(T)$ (in this procedure the delta function in (29) is effectively broadened into a box function $\bar{\delta}(x)$ equal to one inside each bin). Figure 10 plots $P(T)$ for the dirty interface and the two thin slabs. The result is compared to $P_{\rm D}(T)$ of equation (31) and the one which describes the numerical data:

$$P_{\rm fit}(T) = \frac{G}{2G_Q}\frac{1}{T^{3/2}\sqrt{1-T}}. \tag{32}$$

This formula is, up to a numerical factor, the same as the analytical prediction of Schep and Bauer [5] for a single dirty interface:

$$P_{\rm SB}(T) = \frac{G}{\pi G_Q}\frac{1}{T^{3/2}\sqrt{1-T}}, \tag{33}$$

Thus, interfaces belong to a universality class different from that of diffusive bulk conductors characterized by the Dorokhov distribution $P_{\rm D}(T)$. However, it seems that the distribution is valid even for thin slabs whose thickness L is grater than λ_F, but is smaller than the localization radius (which in our case can be estimated in the pedestrian way as the thickness at which conductance vanishes). This is in compliance with experimental confirmation of $P_{\rm SB}(T)$ in a uniform Nb/AlO_x/Nb Josephson junction, whose subharmonic gap structure in the I–V characteristic is extremely sensitive to the number of conducting channels at E_F and their transmission probabilities [64], since the thickness of the realistic AlO_x barrier is bigger than λ_F in the junction electrodes (for example reference [20] gives a simple derivation of the Schep–Bauer distribution without using the assumption $L \ll \lambda_F$). In fact, even our extremely high disorder input in the standard Anderson model generates surface conductance in the band centre, $g_I \simeq 9 \times 10^{10}\ \Omega^{-1}\ {\rm cm}^{-2}$ (for $a = 3$ Å), that is much higher than $10^8\ \Omega^{-1}\ {\rm cm}^{-2}$ reported for the measured value in [20]. This suggests that thin slab is more likely to play to role of a barrier in these Josephson junctions than the strict geometrical plane. While being an intriguing concept in disordered electron physics, universality can be frustrating for the device engineers. Not all features of the transport through dirty interfaces are universal [5].

5. Transport through multilayers

Armed with the knowledge of transport properties of dirty interfaces and metallic homogeneous layers, we can now undertake the study of circuits composed of such elements. The main feature of our circuits is that they are of nanoscale size (a few λ_F) and fully phase coherent

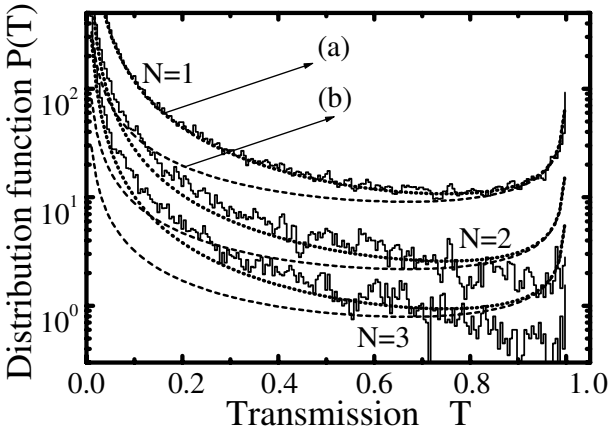

Figure 10. The distribution function $P(T)$ of the transmission eigenvalues (at half-filling $E_F = 0$) for a single disordered interface $N = 1$, and thin slabs composed of two ($N = 2$) or three ($N = 3$) such interfaces, modelled by the Anderson model with $W_I = 30$ on a cubic lattice, $N \times N_y \times N_z$. The disorder average is taken over an ensemble of 1000 conductors. The analytical functions plotted are: (a) $P_{fit}(T) = (G/2G_Q)/(T^{3/2}\sqrt{1-T})$, and (b) the Dorokhov distribution $P(T) = (G/2G_Q)/(T\sqrt{1-T})$.

(i.e., effectively at zero temperature). The choice of disorder and size of the system is driven by the interest here in exploring the patterns of breaking (under the influence of quantum effects) of a simple description of the multilayer in terms of a classical resistor network. Therefore, I study such deviations from semiclassical behaviour by computing the exact zero-temperature conductance of several multilayers, as well as of their components, using the mesoscopic Kubo formula (14). This computation takes into account all quantum interference and quantum-size effects from the outset. In general, resistors can be added according to the classical Ohm's law only when their size is larger than the dephasing length L_ϕ (in this case the quantum features of diffusion can still enter through the transport properties of individual phase-coherent units of size L_ϕ, an example being the weak localization effect [42] at finite temperatures). At high enough temperatures the system can be partitioned into cubes of a macroscopic size L_ϕ where quantum interference between wavefunctions scattered in different cubes can be neglected. This makes it possible then to define an intensive quantity [22], such as conductivity, by solving a classical random resistor network problem [66]. The quantum composition law for quantum resistors in a chain is more complicated, since it contains a phase variable depending on the characteristics of all scatterers [67, 68]. For example, two resistors in a series cannot be added because resistors are not simply voltage biased, and the fluctuating phase across each element $\phi = (e/\hbar)\int v(t)\,\mathrm{d}t$ makes it impossible to infer the properties of a circuit from the conductance of its components [69]. Because of conductance fluctuations [70], generated by quantum interference effects, even homogeneous sample resistance as a function of length is not a self-averaging quantity (therefore requiring disorder averaging to restore the ohmic scaling [21, 71]). In the Landauer–Büttiker scattering formalism, the resistor network description corresponds to a semiclassical concatenation of the scattering matrices of individual units ($\boldsymbol{t}$ in (28) is just one block of a full scattering matrix [62]), i.e., the concatenation of 'probability scattering matrices' of successive disordered regions (obtained by replacing each element of the scattering matrix by its squared modulus [65]).

The multilayers studied here are composed of three bulk conductors joined through two dirty interfaces. The whole structure is modelled by the TBH equation (16) on a $17 \times 10 \times 10$

lattice where the sixth and twelfth monatomic layers contain the same interface as was studied in section 4. The disorder strength within the plane of the interface is fixed at $W_I = 30$, while disorder inside the bulk layers (composed of five monolayers) is varied. The disorder strength is taken to be the same in the two outer layers where the diffusive bulk scattering takes place. This type of multilayer can be viewed as a period of an infinite A/B multilayer [60]: a layer of material A on the outside (of resistivity ρ_A and total thickness $2L_A = 10a$, where a is the lattice spacing) and an interlayer material B between the interfaces (of resistivity ρ_B and thickness $L_B = 5a$). For example, for the chosen disorder strengths $W = 3$ and 6 the corresponding bulk material resistivities at half-filling are $\rho \simeq 130$ and 500 $\mu\Omega$ cm (assuming $a = 3$ Å), respectively. I neglect any potential step at the interface (caused by the conduction band shift at the interface [4]). Such multilayers are often described semiclassically in terms of the resistor model [24]

$$R_{\mathrm{RM}} = N_b\left(\rho_A\frac{2L_A}{S} + \rho_B\frac{L_B}{S} + 2R_I\right), \tag{34}$$

where R_{RM} is the total multilayer resistance, N_b is the number of bilayers (I study below just one multilayer period $N_b = 1$), and R_I is the interface resistance (evaluated in section 4 in figure 9). Thus, the resistor model treats both bulk and interface resistances as semiclassical elements of a circuit in which resistors add ohmically in series. Nevertheless, quantum diffusion can be important inside each individual resistor element, as discussed above [18]. From the measurement of R_{RM} as a function of the layer thickness, the bulk and interface resistances can be extracted experimentally. When quantum interference effects become important in the CPP transport, this picture is expected to break down.

The quantum (i.e., zero-temperature) conductance of the multilayers is computed using a standard tool throughout the paper—the mesoscopic Kubo formula of equation (14) where the whole multilayer is treated as a single phase-coherent unit. This approach intrinsically takes into account finite-size effects in the problem [43], as emphasized in section 2, as well as all single-particle quantum interference effects. In all calculations the hopping integrals throughout the disordered sample and in the leads are the same ($t_{\mathrm{L}} = t_{\mathrm{C}} = t$). This means that no additional scattering, discussed in section 3, is generated at the lead–sample interface [55]. The remaining resistance can sometimes be interpreted as a series addition of two quantum resistors. That is, the semiclassical limit of the two-probe Landauer or Kubo formula for conductance, obtained e.g., from the stationary-phase approximation [72] of the Green function expression (28) for the transmission of the sample, leads to

$$\langle G\rangle^{-1} = R_{\mathrm{QPC}} + \rho\frac{L}{S}, \tag{35}$$

which should be valid for scattering on impurities that is not too strong. The 'contact' resistance [73] $R_{\mathrm{QPC}} = \pi\hbar/e^2N_{\mathrm{ch}}$ is non-zero even for a ballistic conductor because a finite cross-section can carry only finite currents (the voltage drop in this case occurs at the lead–reservoir interface). A similar interpretation was given for the interface resistance [60], and is expected to be valid also for interfaces embedded in a multilayer if there is no coherent scattering between adjacent interfaces (e.g., when such effects are destroyed by sufficiently strong scattering in the bulk). These formulae naturally lead to the resistor model where different interfaces and bulk layers contribute to the CPP resistance as resistors in series. It is often assumed that R_{QPC} can be neglected when compared to the usually much higher resistance of a diffusive sample, thus making the choice of the two-probe (or some other) geometry just a matter of computational convenience [56].

Since the resistor model is expected to be retrieved in the limit of completely diffusive scattering in the bulk and lack of phase coherence [60, 74], in the quest for substantial

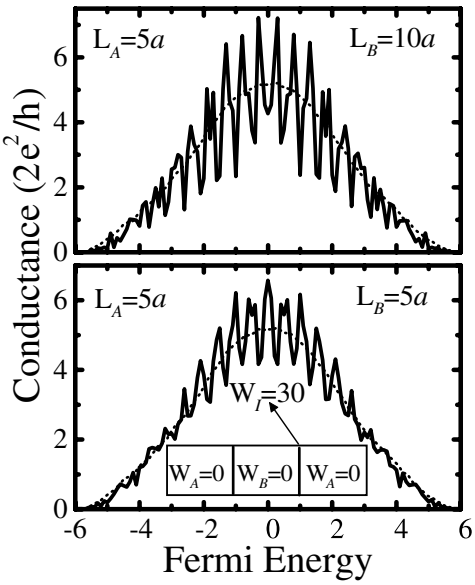

Figure 11. The disorder-averaged (over 200 configurations) conductance of a mesoscopic multilayer, composed of dirty interfaces and clean bulk conductors, modelled on a $17 \times 10 \times 10$ lattice. The results are obtained from the mesoscopic Kubo formula (14) applied to the whole multilayer (solid curve) and from using the semiclassical resistor model, $G_{\mathrm{RM}} = (2R_I - R_{\mathrm{QPC}})^{-1}$ (dotted curve), where individual resistances are computed also from equation (14) and summed accordingly (the meaning of R_{QPC} is explained in figure 15).

quantum-effect-induced deviations from this picture I start from the opposite limit: a multilayer composed of clean (ballistic) layers and disorder introduced only on the interfaces, $W_A = W_B = 0$ and $W_I = 30$. The disorder-averaged result is plotted in figure 11 for two different thicknesses of the interlayer. Even after disorder averaging, the conductance oscillates as a function of E_F. This clearly quantum effect is a consequence of the size quantization caused by a coherent interference of electrons reflected back and forth at the strongly disordered interface. After adding the disorder into the outer layers, the effect persists, albeit with a smaller amplitude of oscillations (figure 12). However, while this is plausible because of the interlayer being composed of only a few atomic monolayers [4] (i.e., its length is of the order of λ_F), it is somewhat surprising that oscillations increase with increasing separation between the interfaces. Furthermore, the oscillating conductance is still quite different from the pure resonant tunnelling conductance peaks which would occur at the energies of bound states if interfaces were replaced by the tunnelling barriers [18] (e.g., in our model this can be generated by reducing the hopping integral t_{mn} between the outer layers and the interlayer [55]). Although it is obvious that this phenomenon cannot be accounted for by the semiclassical resistor model, our findings are plotted for the sake of comparison. Also, by adding impurities in the interlayer we can follow the disappearance of conductance oscillations (which is akin to studies of disorder effects on conductance quantization in ballistic conductors [46]). The effect has almost vanished at $W = 2$ although the mean free path, e.g., around the band centre, $\ell \approx 9$ (obtained from the Bloch–Boltzmann equation with the Born approximation for the scattering on a single impurity [21]) is still larger than L (i.e., the transport within the interlayer has not yet reached the limit of fully diffusive bulk scattering).

To sweep through the transitional region between fully quantum and (expected) resistor model semiclassical description, a disorder is introduced in both layers A and B. The results

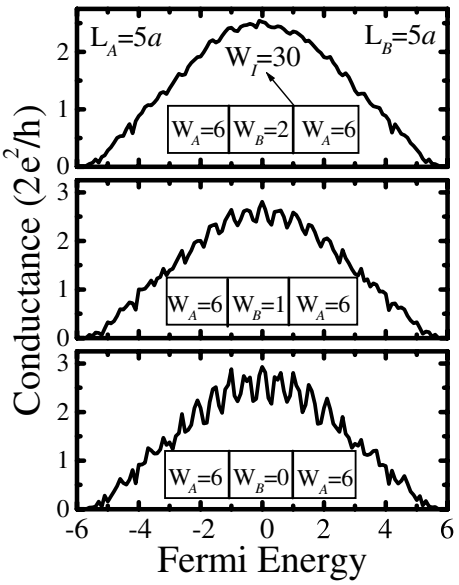

Figure 12. The disorder-averaged (over 200 configurations) conductance of a mesoscopic multilayer, composed of strongly disordered interfaces and (quasi)ballistic bulk conductors (e.g., $\ell \approx 9$ at half-filling for $W = 2$), modelled on a $17 \times 10 \times 10$ lattice. The results are obtained from the mesoscopic Kubo formula (14) applied to the whole multilayer as a single quantum-coherent conductor.

are shown in figures 13 and 14. The disorder $W = 6$ is the strongest one in the Anderson model where one can still use the semiclassical picture of transport at half-filling (i.e., at $E_F = 0$ we get [21] $\ell \sim a$ for $W \simeq 6$, but localization is postponed to much higher values of [61] $W \simeq 16.5$). The other type of homogeneous layer is modelled with $W = 3$, which is at the crossover between the ballistic and the diffusive transport regime, since $\ell \approx 4$ at $E_F = 0$ and $L_A = L_B = 5a$. The statistical error bars on the disorder-averaged conductance (over $N_{\rm conf}$ samples), defined as $\Delta G = \sqrt{\mathrm{Var}\, G/N}$, are smaller than the size of the dots (this further clarifies that small conductances of the multilayers are not the consequence of strong disorder, but are generated by combining a few metallic resistors and dirty interfaces in a series). The conductances of individual layers are plotted in figure 15. In the first case $W_A = W_B = 3$, the naive application of the resistor model, where $R_{\rm QPC}$ is neglected, leads to $G'_{\rm RM}$ ($G_{\rm RM} = 1/R_{\rm RM}$ is the sum of component resistances) being smaller than the quantum G computed for the multilayer as a single coherent unit. However, the subtraction of four $R_{\rm QPC}$, which brings $G_{\rm RM}$ into the form of equation (35), gives conductance higher than $G_{\rm RM} > G$. Here $R_{\rm QPC}$ is the resistance of a ballistic conductor ('quantum point contact') with a cross-section $A = 100a^2$ (see figure 15). According to equation (35), the resistances of homogeneous layer components of the multilayer, which are plotted in figure 15 (or figure 9 for the interface alone), are the sums of their 'intrinsic bulk' resistance [56] and $R_{\rm QPC}$. Thus, when adding these resistors, the final sum should contain only one $R_{\rm QPC}$ if the resistor model is to be compared with the two-probe resistance of the multilayer. In all other cases which include a layer with diagonal disorder $W = 6$, both naive and more careful attempts (where $(N_R - 1)$ contact resistances $R_{\rm QPC}$ are subtracted from the sum of the resistances of component layers, where N_R is the number of bulk and interface resistances used to obtain such a sum) to use the resistor model give conductances which are greater than the ones computed for the

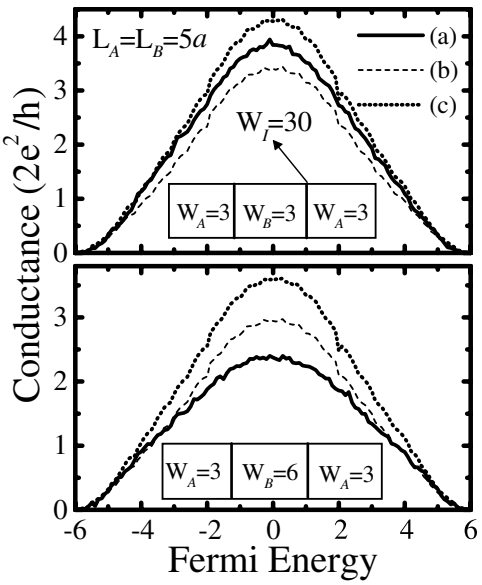

Figure 13. The disorder-averaged (over 200 configurations) conductance of a mesoscopic multilayer, composed of strongly disordered interfaces and weakly disordered bulk conductors, modelled on a $17 \times 10 \times 10$ lattice ($\ell \approx 4a$ at half-filling for $W = 3$). The results are obtained from: (a) the mesoscopic Kubo formula (14) evaluated for the whole multilayer, following the resistor model equation (34); (b) $G'_{\rm RM} = (2R_A+R_B+2R_I)^{-1}$; and (c) $G_{\rm RM} = (2R_A+R_B+2R_I-4R_{\rm QPC})^{-1}$.

multilayer as a single conductor. The explanation which invokes only extra scattering on the boundaries between different components inside the multilayer, which does not work in the first case $W_A = W_B = 3$, is not the only one possible.

It was shown recently [21] that even in weakly disordered metals (where the Boltzmann resistivity is practically indistinguishable from the one computed from the Kubo formula), clear separation of a two-probe resistance into a contact term and diffusive bulk resistance, as implied by the standard arguments of equation (35), is tempered by localization effects (i.e., terms of the order of ℓ/L which are neglected in equation (35)), and therefore possible only in very weakly disordered systems. To elucidate the effects responsible for the difference between the two ways of evaluating the multilayer conductance in figures 13 and 14, I apply the same analysis to a multilayer where dirty interfaces are removed (i.e., $\varepsilon_m = 0$ on the sixth and twelfth plane along the x-axis). When $W_A \neq W_B$, such multilayers are similar to the junction studied in section 3 where the interface is not explicitly modelled as in section 4, but appears as a boundary between two different homogeneous materials brought into contact. In the opposite case $W_A = W_B$, the sample is akin to the homogeneously disordered conductor whose conductance was studied in figure 7. The results of these calculations, plotted in figures 16 and 17, hint that the difference between the resistor model conductance $G_{\rm RM}$ and the conductance G of the multilayer as one indivisible quantum-coherent unit is quite minuscule, with the proviso that extraneous contact resistance terms are properly subtracted. Even though the multilayers are mesoscopic, where electrons retain their phase coherence and are subject thereby to quantum interference effects, disorder averaging effectively destroys most of the random interference terms (a sample self-averages at finite temperatures when it can be partitioned into a cubes of size L_ϕ, as discussed above) [75]. The surviving interference terms are exemplified by those generated by quantum interference effects on special trajectories (i.e., Feynman paths), such as the closed loops

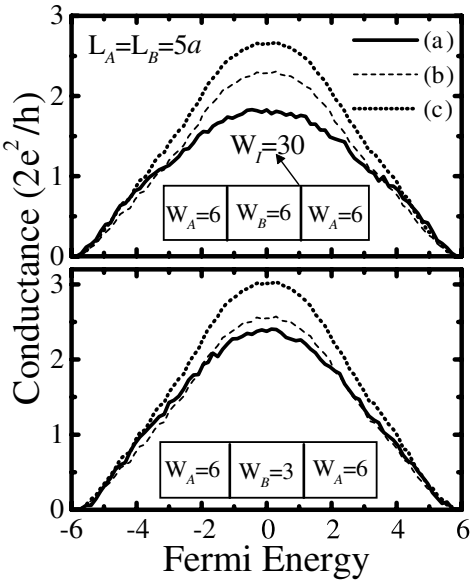

Figure 14. The disorder-averaged (over 200 configurations) conductance of a mesoscopic multilayer, composed of strongly disordered interfaces and weakly disordered bulk conductors, modelled on a $17 \times 10 \times 10$ lattice. The results are obtained from: (a) the mesoscopic Kubo formula (14) evaluated for the whole multilayer, following the resistor model equation (34); (b) $G'_{\rm RM} = (2R_A + R_B + 2R_I)^{-1}$; and (c) $G_{\rm RM} = (2R_A + R_B + 2R_I - 4R_{\rm QPC})^{-1}$.

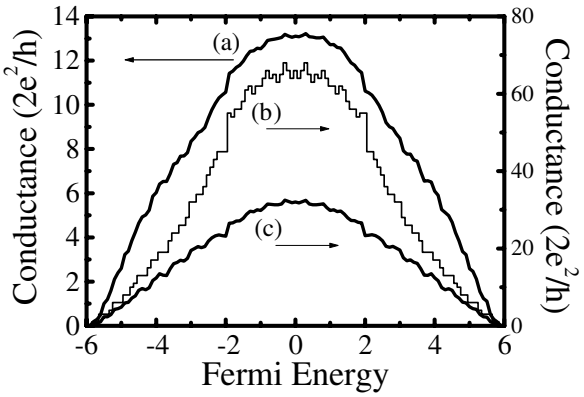

Figure 15. Conductance of individual resistors comprising the multilayers of section 5: disordered conductors modelled by the Anderson model $5 \times 10 \times 10$ lattice with diagonal disorder strength (a) $W = 6$, and (c) $W = 3$, and quantum point contact conductance $(1/R_{\rm QPC})$ for a clean sample modelled on the lattice with the same cross-section (i.e., on a lattice supporting 100 conducting channels, where the maximum number of open channels with $T_n = 1$ at the Fermi level in such 3D ballistic conductors [55] is 68 at $|E_F| \simeq 0.3$).

responsible for weak localization [76]. These non-local weak localization effects, arising from the interference between the amplitudes along the conjugated time-reversed loops which span the whole phase-coherent sample, are responsible for G being slightly smaller than $G_{\rm RM}$ (localization effects inside the individual resistors are taken into account even by the resistor model prescription). As expected in this picture, the discrepancy is very small at $W = 3$,

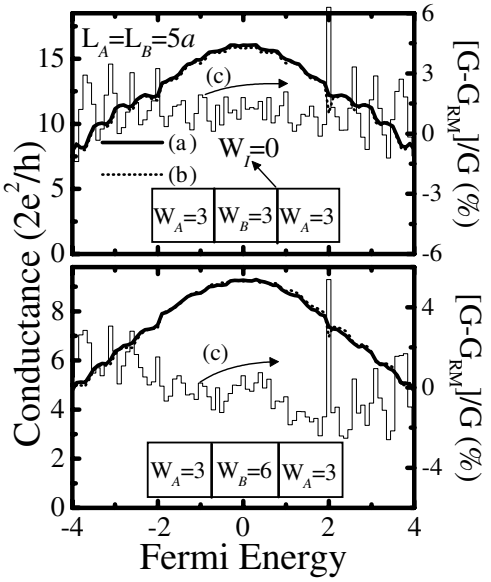

Figure 16. The disorder-averaged (over 200 configurations) conductance of a mesoscopic multilayer, composed of strongly disordered interfaces and weakly disordered bulk conductors, modelled on a $17 \times 10 \times 10$ lattice. The results are obtained: (a) from the mesoscopic Kubo formula (14) evaluated for the whole multilayer; and (b) following the resistor model equation (34), $G_{\mathrm{RM}} = (2R_A + R_B - 2R_{\mathrm{QPC}})^{-1}$. The relative error $[G - G_{\mathrm{RM}}]/G$ is plotted as (c).

and increases for stronger disorder [21] $W = 6$. On the other hand, conductance fluctuations 'sneak in' through the fluctuations of the relative error $[G - G_{\mathrm{RM}}]/G$ of the resistor model as a function of Fermi energy (cf figures 16 and 17).

6. Conclusions

I have studied different macroscopically inhomogeneous disordered 3D conductors of nanoscale size by employing both a fully quantum description, provided by the mesoscopic two-probe Kubo formula, and a semiclassical resistor model. Before embarking on the technicalities of computations some fundamental issues in the quantum transport theory were scrutinized: the relationship between the Kubo formula in the exact single-particle eigenstate representation and the Kubo formula for the finite-size sample inspired by mesoscopic physics; the influence of the macroscopic leads ('measuring apparatus') on the computed two-probe conductance; and the transmission and transport properties of a single dirty interface, which are markedly different from standard notions developed for bulk conductors. It was shown, by exact computation for examples of homogeneous disordered samples and inhomogeneous metal junctions, that the mesoscopic Kubo formula allows one to obtain reliable results for the static zero-temperature conductance (which includes the properties of the attached leads) characterizing non-interacting quasiparticle transport. On the other hand, the evaluation of the traditional Kubo formula, based on the exact diagonalization of the respective Hamiltonian, ends up with a numerical discrepancy when compared to mesoscopic methods applied to homogeneous samples (because of the necessity of handling small numerical parameters, such as the width of the Lorentz-broadened delta function). Moreover, this traditional technique fails completely in the case of macroscopically inhomogeneous (junctions and multilayers)

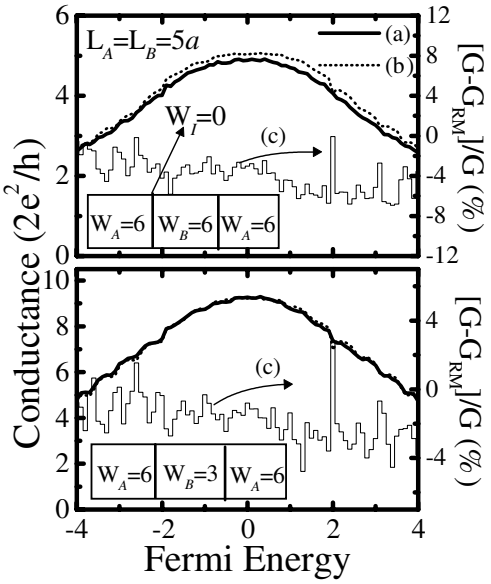

Figure 17. The same calculation as in figure 16 (the same labels apply), but for a slightly different multilayer where the disorder strength is increased to $W = 6$ in the two outer layers.

samples. This can be traced back to the conceptual obstacles in applying methods derived for an infinite sample to a finite-size system (even after it has been extended through using periodic boundary conditions) where the problem of dissipation and the effect of the sample boundaries (which is crucial for the description of mesoscopic devices) are bypassed for the sake of computational pragmatism.

The study of a single dirty interface, with specific Anderson-model-type disorder, shows that its transmission properties are well accounted for by the Schep–Bauer distribution, but this formula applies approximately also to thin slabs composed of a few such interfaces (which is important for experimental investigations where one hardly deals with the geometrical planes of theoretical analysis). The nanoscale mesoscopic multilayers containing such interfaces and ballistic bulk conductors exhibit disorder-averaged oscillating conductance as a function of Fermi energy. This effect of the phase coherence and quantum-size effect is slowly destroyed upon adding the disorder inside the layers. However, even for diffusive scattering in the metallic layer components, smooth disorder-averaged multilayer conductances cannot be completely accounted for by the resistor model (which sums layer and interface resistances as resistors connected in series). Since this classical approach works well when interfaces are removed (up to tiny localization effects arising from interference effects inside the whole sample), we can conclude that just a single plane of a strongly disordered material is enough to bring new quantum effects into the conductance of mesoscopic metallic multilayered structures.

Acknowledgments

I am grateful to P B Allen for guidance and an unlimited supply of intriguing questions, and to I L Aleiner and J A Vergés for valuable discussions. This work was supported in part by NSF grant no DMR 9725037.

References

[1] Baibich M N, Broto J M, Fert A, Nguyen Van Dau F, Petroff F, Etienne P, Creuzet G, Friederich A and Chazelas J 1988 *Phys. Rev. Lett.* **61** 2472
[2] Binasch G, Grünberg P, Saurenbach F and Zinn W 1989 *Phys. Rev.* B **39** 4828
[3] Dugaev V K, Litvinov V I and Petrov P P 1995 *Phys. Rev.* B **52** 5306
[4] Gijs M A M and Bauer G E W 1997 *Adv. Phys.* **46** 286 and references therein
[5] Schep K M and Bauer G E W 1997 *Phys. Rev.* B **56** 15 860
[6] Fan H Y 1942 *Phys. Rev.* **61** 365
Fan H Y 1942 *Phys. Rev.* **62** 388
[7] Fuchs K 1938 *Proc. Phil. Camb. Soc.* **34** 100
[8] Sondheimer E H 1952 *Adv. Phys.* **1** 1
[9] Zhang X-G and Butler W H 1995 *Phys. Rev.* B **51** 10 085
[10] Akkermans E, Pichard J-L and Zinn-Justin J (ed) 1995 *Mesoscopic Quantum Physics (Les Houches Session LXI)* (Amsterdam: North-Holland)
[11] Landauer R 1957 *IBM J. Res. Dev.* **1** 223
Landauer R 1970 *Phil. Mag.* **21** 863
Büttiker M 1986 *Phys. Rev. Lett.* **57** 1761
[12] Bauer G E W, Brataas A, Schep K and Kelly P 1994 *J. Appl. Phys.* **75** 10
[13] Bauer G E W 1992 *Phys. Rev. Lett.* **69** 1676
[14] Asano Y, Oguri A and Maekawa S 1993 *Phys. Rev.* B **48** 6192
[15] Caroli C, Combescot R, Nozières P and Saint-James D 1971 *J. Phys. C: Solid State Phys.* **4** 916
Meir Y and Wingreen N S 1992 *Phys. Rev. Lett.* **68** 2512
[16] Nikolić B K 2001 *Phys. Rev.* B **64** 165303
[17] Sanvito S, Lambert C J, Jefferson J H and Bratkovsky A M 1999 *Phys. Rev.* B **59** 11 936
[18] Datta S 1995 *Electronic Transport in Mesoscopic Systems* (Cambridge: Cambridge University Press)
[19] Kramer B and MacKinnon A 1993 *Rep. Prog. Phys.* **56** 1469
[20] Naveh Y, Patel V, Averin D V, Likharev K K and Lukens J E 2000 *Phys. Rev. Lett.* **85** 5404
[21] Nikolić B K and Allen P B 2001 *Phys. Rev.* B **63** R020201
[22] Janssen M 1998 *Phys. Rep.* **295** 1
[23] Rammer J 1998 *Quantum Transport Theory* (Reading, MA: Perseus Books)
[24] Zhang S and Levy P M 1991 *J. Appl. Phys.* **69** 4786
[25] Stein J and Krey U 1980 *Z. Phys.* B **37** 13
[26] Lee P A and Ramakrishnan T V 1985 *Rev. Mod. Phys.* **57** 287
[27] Baranger H U and Stone A D 1989 *Phys. Rev.* B **40** 8169
Nöckel J U, Stone A D and Baranger H U 1993 *Phys. Rev.* B **48** 17 569
[28] Efetov K B 1997 *Supersymmetry in Disorder and Chaos* (Cambridge: Cambridge University Press)
[29] Payne M C 1989 *J. Phys.: Condens. Matter* **1** 4931
[30] Nazarov Yu V 1994 *Phys. Rev. Lett.* **73** 134
[31] Kane C L, Serota R A and Lee P A 1988 *Phys. Rev.* B **37** 6701
[32] Kane C L, Lee P A and DiVincenzo D P 1988 *Phys. Rev.* B **38** 2995
[33] Stone A D 1995 *Mesoscopic Quantum Physics (Les Houches Session LXI)* (Amsterdam: North-Holland)
[34] Nikolić B and Allen P B 1999 *Phys. Rev.* B **60** 3963
[35] Abrahams E, Anderson P W, Licciardello D C and Ramakrishnan T V 1979 *Phys. Rev. Lett.* **42** 673
[36] Berkovits R, Kantelhardt J W, Avishai Y, Havlin S and Bunde A 2001 *Phys. Rev.* B **63** 085102
[37] Calandra M and Gunnarsson O 2001 *Phys. Rev. Lett.* **87** 266601
[38] Feldman J L, Kluge M D, Allen P B and Wooten F 1993 *Phys. Rev.* B **48** 12 589
[39] Kubo R, Miyake S I and Hashitsume N 965 *Solid State Physics* vol 17, ed F Seitz and D Turnbull (New York: Academic) p 288
[40] Economou E N 1990 *Green's Functions in Quantum Physics* 2nd edn (Berlin: Springer)
[41] Thouless D J and Kirkpatrick S 1981 *J. Phys. C: Solid State Phys.* **14** 235
[42] Gor'kov L P, Larkin A I and Khmel'nitskii D E 1979 *Pis. Zh. Eksp. Teor. Fiz.* **30** 248 (Engl. transl. 1979 *JETP Lett.* **30** 228)
[43] Imry Y and Landauer R 1999 *Rev. Mod. Phys.* **71** S306
[44] Fisher D S and Lee P A 1981 *Phys. Rev.* B **23** 6851
[45] Zhang X-G and Butler W H 1997 *Phys. Rev.* B **55** 10 308
[46] Szafer A and Stone A D 1989 *Phys. Rev. Lett.* **62** 300
[47] Cuevas J C, Levy Yeyati A and Martín-Rodero A 1998 *Phys. Rev. Lett.* **80** 1066

[48] Press W H, Teukolsky S A, Vetterling W T and Flannery B P 1992 *Numerical Recipes in FORTRAN* 2nd edn (Cambridge: Cambridge University Press)
[49] Vergés J A 1998 *Phys. Rev.* B **57** 870
[50] Prelovšek P 1978 *Phys. Rev.* B **18** 3657
[51] Wegner F 1980 *Z. Phys.* B **36** 209
[52] Anderson P W 1997 *The Theory of Superconductivity in the High-T_c Cuprates* (Princeton, NJ: Princeton University Press) p 158
[53] Landauer R 1987 *Z. Phys.* B **68** 217
[54] Weidenmüller H A 1990 *Physica* A **167** 28
[55] Nikolić B K and Allen P B 2000 *J. Phys.: Condens. Matter* **12** 9629
[56] Braun D, Hofstetter E, MacKinnon A and Montambaux G 1997 *Phys. Rev.* B **55** 7557
[57] Pratt W P Jr, Lee S-F, Slaughter J M, Loloee R, Schroeder P A and Bass J 1991 *Phys. Rev. Lett.* **66** 3060
Gijs M A M, Lenczowski S K J and Giesbers J B 1993 *Phys. Rev. Lett.* **70** 3343
[58] Stiles M D and Penn D R 2000 *Phys. Rev.* B **61** 3200
[59] Yang Q *et al* 1995 *Phys. Rev.* B **51** 3226
Lee S-F *et al* 1995 *Phys. Rev.* B **52** 15 426
[60] Schep K M, van Hoof J B A N, Kelly P J, Bauer G E W and Inglesfield J E 1997 *Phys. Rev.* B **56** 10 805
[61] Slevin K, Ohtsuki T and Kawarabayashi T 2000 *Phys. Rev. Lett.* **84** 3915
[62] Beenakker C W J 1997 *Rev. Mod. Phys.* **69** 731
[63] Dorokhov O N 1984 *Solid State Commun.* **51** 381
[64] Bardas A and Averin D V 1997 *Phys. Rev.* B **56** R8518
[65] Cahay M, McLennan M and Datta S 1988 *Phys. Rev.* B **37** 10 125
[66] Kaveh M and Moth N F 1987 *Phil. Mag.* B **55** 9
[67] Anderson P W, Thouless D J, Abrahams E and Fisher D S 1980 *Phys. Rev.* B **22** 3519
[68] Büttiker M 1986 *Phys. Rev.* B **33** 3020
[69] Levy Yeyati A, Martín-Rodero A, Esteve D and Urbina C 2001 *Phys. Rev. Lett.* **87** 046802
[70] Al'tshuler B L 1985 *Pis. Zh. Eksp. Teor. Fiz.* **41** 530 (Engl. transl. 1985 *JETP Lett.* **41** 648)
Lee P A and Stone A D 1985 *Phys. Rev. Lett.* **55** 1622
[71] Todorov T N 1996 *Phys. Rev.* B **54** 5801
[72] Baranger H U, DiVincenzo D P, Jalabert R A and Stone A D 1991 *Phys. Rev.* B **44** 10 637
[73] Sharvin Yu V 1965 *Zh. Eksp. Teor. Fiz.* **48** 984 (Engl. transl. 1965 *Sov. Phys.–JETP* **21** 655)
[74] Bozec D, Howson M A, Hickey B J, Shatz S, Wiser N, Tsymbal E Y and Pettifor D G 2000 *Phys. Rev. Lett.* **85** 1314
[75] Altshuler B L and Simons B D 1995 *Mesoscopic Quantum Physics (Les Houches Session LXI)* (Amsterdam: North-Holland)
[76] Larkin A I and Khmel'nitskii D E 1982 *Usp. Fiz. Nauk* **136** 536 (Engl. transl. 1982 *Sov. Phys.–Usp.* **25** 185)
Khmel'nitskii D E 1984 *Physica* B **126** 235